Evolution of fire models for estimating structural fire-resistance

Aatif Ali Khan[1], Asif Usmani[1], José Luis Torero[2]

[1]*Department of Building Services Engineering, The Hong Kong Polytechnic University, Kowloon, Hong Kong*

[2]*Department of Civil, Environmental & Geomatic Engineering, University College London, London, UK*

Abstract

Many fire models have been proposed to investigate structural response to fire, where fire is considered as a structural "load" and the structural response determines the "resistance" offered by the structure. Where the term "resistance" is used with its physical meaning and is not restrained by its standard application. Over the course of time, fire models have evolved from simply using the highest gas temperatures resulting from a fully developed compartment fire to more sophisticated computational fluid dynamics (CFD) models, where hyper-realistic time-varying structural temperatures can be determined for a range of realistic fire scenarios. This paper examines the current state of the art in terms of defining gas temperatures for structural fire analysis. Widely adopted fire models used in structural analysis are therefore reviewed. This paper discusses the limitations and scope of applicability of the most commonly used fire models. Recent developments on the coupling of CFD and FEM models are also discussed in detail and their applicability to practical fire scenarios is explored. The primary concern of this review is to evaluate the fire models for their suitability while using for structural fire assessment and not to review studies on the manner in which the actual structural assessment is done.

Keywords – fire modes, CFD, FEM, structural engineering, coupling, review

1. Introduction

Over the past seven decades, exhaustive studies have been conducted to understand the structural response to different kinds of fire scenarios such as compartment fires, localised fires and "travelling" fires [1]. Most of the models used so far assume fully developed fires based on the assumption that the evaluation of structural fire resistance is really only required for post flashover fires. However, as experience of real fires has accumulated, models for localised or "travelling" fires have been increasingly used, where the fire may be in a pre-flashover or spreading regime. The data used to develop these fire models is mainly based on experimental studies resulting in empirically derived correlations to quantify the models. Analytical and numerical models have also been developed, based on idealisations of the fire compartment, such as zone models. Recent trend toward performance-based engineering (PBE) approaches is beginning to require even more accurate representations of fires and consequently more realistic boundary conditions for fire exposed structural components, leading to greater use of computational models. In this context it is becoming important to understand the origin, scope and limitations of the most commonly used fire models used to establish a "fire load" for structural analysis, so that the best possible choice can be made for the problem at hand.

A comprehensive study of fire testing to analyse the interaction between fire and structural elements is conducted by Bisby et al. [2]. The interaction of fire with a solid is a complex engineering problem. To

acquire an accurate solution, researchers have proposed methods which are usually simplified to address specific fire scenarios by introducing suitable assumptions and limiting the scope of such methods to those specific fire scenarios. Studies have further established that extending the use of these fire models to other scenarios may be questionable. The earliest approach comes from research that led to the development of the standard "temperature-time" curve [3], which is most commonly used as the "fire-load" in structural design, although it is well known that the curve does not represent a real fire. The standard "temperature-time" curve has led to a generalized link between the term "fire resistance" and exposure to the standard "temperature-time" curve as the "fire load." While it is recognized that this link might lead to confusion, it is important to retain the terminology "fire resistance" as a representation of the response of the structure to any "fire load." The initial work of Kawagoe [4] and Thomas [5] pioneered the development of the relationship of fire with the geometry of compartments resulting in the first alternative definition of the "fire load." This directed researchers towards conducting more refined studies to refine and validate the models developed by them.

A detailed study of fire models can be found in the SFPE handbook [6] for both pre-flashover and post-flashover fire scenarios. SFPE Task Group on Fire Exposures to Structural Elements developed the SFPE Engineering Guide for Fire Exposure to Structural Elements [7] followed by Engineering Standard on Calculating Fire Exposures to Structures [8], these guides provide a detailed review of numerous methods used for calculating structural response to fire. In recent years, more sophisticated models have been developed which are based on CFD. CFD provides greater resolution (spatial and temporal) of the thermal boundary conditions over structural surfaces. However, because of difference in spatial and temporal resolution of the fire and the structural domains, it is a challenging task to couple a CFD model with finite element methods (FEM) for simultaneous or coupled simulations of both the fire and the structural response.

Although, both numerical and experimental models have evolved resulting in greater understanding of fire behaviour, there are still no generalised models that could be used for all fires. Furthermore, the capabilities and limitations of existing approaches have not been explored in a systematic manner. This paper examines and reviews the evolution of fire models as it pertains their use in determining structural response to fire and tries to answer the following three essential questions for each model considered: (1) what are the assumptions and simplifications? (2) what are the limitations? and (3) in what kind fire-scenarios is the model applicable? Once these three questions are answered, structural engineers can use these models in an appropriate manner and focus on establishing the necessary performance requirements for structures exposed to fire.

2. Formulation of the Problem

When implementing a fire model for the purpose of structural analysis it is necessary to determine the evolution in time of the net energy input from the fire to the structure [9]. This will enable the determination of the time varying temperature change of the structure and the detailed temperature gradients within the structural components to the desired resolution. The net energy input needs to be assessed throughout the duration of the fire, i.e. time to burn-out (t_{BO}), and through the cooling period until the structure has reached ambient temperature (t_{CD}). The time to burn out (t_{BO}) is defined by the amount of fuel available ($M"_F$ $[kg/m^2]$) and the burning conditions (i.e. ventilation and geometry of the compartment) and the time to cool down (t_{CD}) is defined by the conditions within the compartment after the fire has consumed all the fuel (or has been extinguished by firefighters) and the thermal mass of the structure itself. The amount of

fuel available ($M"_F$ $[kg/m^2]$) is therefore an essential input to the analysis and it is generally defined in statistical terms [10,11] for different occupancies.

The net energy input is defined by means of a boundary condition between the structural element and the gas phase. Within the structural elements, conduction heat transfer enables the transport of energy throughout the structure and the quantitative determination of structural temperatures and temperature gradients within the structure. The boundary condition is probably the most complex aspect of the analysis and it has been the subject of many studies. The definition of the boundary condition is a function of the model being used and the assumptions and simplifications embedded in such models. This applies during both heating and cooling regimes. The subsequent sections will focus on this aspect of the problem.

3. Complexity of the Fire Structure Interface

As discussed above, to evaluate the structural response to fire, the key complexity is to acquire the temporal and spatial evolution of proper thermal boundary conditions for structural analysis. Without reliable inputs from a given fire scenario, it is not possible to estimate accurate thermal and mechanical response of structures to fire.

Some of the key issues that need to be resolved when establishing the "fire load" to be used when performing structural analysis for a given fire scenario are as follows:

- Defining reasonable boundary conditions for heat transfer. It is not uncommon that incorrect boundary conditions are used without fully understanding the physics embedded in the heat transfer analysis (convective and radiative heat transfer). Such is the case of the standard fire curve, when a homogenous temperature is assumed throughout the boundary with a prescribed evolution in time. This approach does not represent the realistic thermal load imposed on the structure in a real fire.
- The temperatures within the gas phase around a structural component change significantly faster than the temperature variation in the solid phase. While the thermal response of a structure depends on the thermal properties of the structural material, the time that characterizes the evolution of the gas temperatures will always be much shorter than the characteristic time for the solid phase. This difference plays a critical role on the choice of time step for coupled modelling [9].
- The duration of the fire plays a vital role while defining the severity of fire, and the evolution of the boundary condition needs to be carefully assessed throughout the duration of the fire including the decay period (cooling phase).
- The geometry of the compartment establishes the burning conditions (ventilation, energy distribution, rate of fuel consumption, etc.) which may follow a pattern of growth, steady burning and decay or might never achieve a steady phase. Therefore, the distribution of the fuel is one of the factors that influence the burning conditions. Therefore, the evolution of the burning conditions must be tracked.

4. Fuel Load

The "fuel load" is one of the most decisive parameters to evaluate the structural response to fire, since it governs the amount of heat that can potentially be generated within the compartment. It strongly influences the maximum temperature reached within the compartment and the duration of the fire. Therefore, it is imperative to quantify it rationally. Generally, fuel load density depends on the occupancy classes such as business occupancy, assembly occupancy, hospital, etc. However, uncertainty about fuel load increases

with the time of use (entropy) and may require regular surveys to obtain reliable bounds for fuel load for each occupancy. Over the past century, a few methods have been established to quantify the fuel loads in a compartment that are discussed in subsequent paragraphs.

4.1. Classical surveys

One of the earliest and most comprehensive work to quantify the fuel loads in a compartment was published by Ingberg et al. [12]. A report was produced based on the surveys conducted between 1928 to 1940 for various occupancies. Ingberg's report provided the fuel load per unit floor area for several occupancies (apartments and residences, hospitals, schools, mercantile occupancies, manufacturing establishments, printing plants, warehouses, and offices). The author considered a number of factors while analysing the survey data such as fuel load for different floor areas for the same occupancies and estimation of the contents of closets etc. Moreover, weight of combustibles was measured and expressed in terms of equivalent calorific values of wood and paper. However, since then staggering changes have occurred such as the advent of computers in almost all type of occupancies, advance equipment in hospitals (high content of chemicals and plastics and more complex materials), every-increasing use of polymers, and similar changes in other occupancies as well. Therefore, Ingberg's data is inappropriate for contemporary fire scenarios.

Design values of the fuel load density are generally assigned by performing a statistical study of the surveyed data. A few common approaches are employed during surveys i.e. direct weighing method (involving weighing all combustibles inside the compartment); inventory method (indirect calculation of the mass using volume and density of the material); and questionnaire (a qualitative analysis). A number of surveys have been carried out so far however only a handful in the last two decades. Furthermore, only in a few surveys the compartment size and its usage had been recorded.

In one of the most comprehensive studies by Culver [13] (23 office buildings in US) in the 1970s for office buildings, it was concluded that fuel load density is strongly influenced by the floor area and the purpose of the room. Moreover, using the inventory method, Culver concluded that the life span of the building does not affect the fuel load density. However, life of the building would impact the structural integrity when exposed to fire [14] as during the lifetime of a building, it may suffer deterioration due to environmental and operational conditions as well as due to natural and unnatural shocks. Other statistical studies using different survey methods can be found in references [15–18]. However, all of these surveys have their own advantages and disadvantages for example the weighing method requires skilful and experienced personnel to collect data. Similarly, for inventory methods it is required to have detailed database (catalogues) of equipment and furniture. Moreover, most of these surveys (other than Ingberg et al. [12]) focused on office buildings and the calorific value of the fire load was expressed in terms of equivalent amount of wood or cellulose.

A report by Thomas [19] was published in 1986, it included data from almost all surveys from different countries available at that time. The report included mean and standard deviation for the fuel density obtained from the surveys. For some of the occupancies in the European and Swedish data, fractile value of fuel density was presented. To calculate the design fuel density, a number of factors were included in the calculation as shown in Equation 1. A similar equation can be found in Eurocode 1 (which is described later).

Pettersson et al. [20] also explored the subject of fuel load. Based on a statistical investigation (in Sweden), the authors provided a minimum and maximum magnitude for the fuel load. They recommended a value for the fuel load that can be applied for 80% of the cases of the same type of occupancy. It is worth noting

that the values provided in their study included only furniture and fittings in each occupancy such as dwelling, school, office buildings, hospitals, and hotels. However, the potential fuel load from wall linings and flooring were not included, therefore it must be carefully assessed or evaluated by the designer. However, they suggested a strict and rigorous method to calculate the fuel load in any building by employing the relationship of the fuel load with the combustion efficiency of any fuel (Equation 1). Where mass (m_i) of each material is measured and multiplied with its calorific value (H_i).

$$q = \frac{\sum \mu_i m_i H_i}{A_T} \quad (1)$$

where 'i' represents the *i-th* material and μ_i is the degree of combustion which varies between zero and one. μ_i could be defined only on the basis of fitting to a sufficiently large experimental data base. Failing that, generally it is taken as 1, which may sometimes overestimate the energy released by the fuel load in a compartment.

4.2. Eurocode 1

Eurocode 1 [11] quantifies the design load by providing the mean and fractile values of the characteristic fuel load per unit floor area for different occupancies. The source data [19] from the Eurocode provides a deterministic value for each occupancy that is not influenced by the use of the compartments or has any relationship with the floor area. This is despite, floor area having been shown to have a significant influence on the average fuel load. Culver's survey data [13] for office buildings showed that the fuel load density was higher for smaller floor areas than for large open floor areas. It was also concluded that usage of the room is critical to quantifying the realistic fuel load. For example, rooms used for filing and storage have much higher fuel load density than general office or clerical rooms. Therefore, the design values (Equation 2) [$q_D \; in \; MJ/m^2$] from the Eurocode will inevitably overestimate the fuel load for some scenarios (low density areas) and underestimate for other areas (high-density areas).

$$q_D = q_K . m . \delta_{q1} \delta_{q2} \delta_1 \ldots \ldots \delta_n \quad (2)$$

In Equation 2, q_K (MJ/m^2) represents the characteristic fuel load density per unit floor area of any material (or combination). m, is the combustion factor, generally taken as 0.8 for cellulosic materials. Characteristic fuel loads can be calculated using Equation 3. The various factors presented in Equation 2 are described in Table 1.

$$q_K = \frac{1}{A} \sum M_i \, H_i \psi_i \quad (3)$$

where M_i (kg) is the mass of a material and H_i (MJ/kg) is the calorific value of the material which depends on the moisture content [1,11]. ψ represents a factor that defines if the material is protected or not. A (m^2) is the floor area of the compartment.

Although the Eurocode provides a deterministic value, it includes in that value a number of factors that can alter the design fuel load (q_D) within a compartment.

As can be seen from Equations (2) and (3), the fuel load can be significantly modified by the presence of factors δ_i and ψ_i. The modifications are so significant that specific sets of modifications can alter the outcome from extreme fire proofing requirements to very mild or no fire proofing requirements. Therefore, these constants deserve more attention. The Eurocode Annex E provides some guidance, but this information is not clearly contextualized or detailed. Table 1 provides the coefficients as presented in

Appendix E of the Eurocode. As explained above, products of the coefficients of δ_i and ψ_i can drastically change the fuel load.

The principle behind Equation (3) is that M_i follows a probabilistic distribution obtained from a survey [19]. This probabilistic distribution may be determined from an independent survey, however, it is more likely that the practitioner will use the recommended values. If the value of M_i is treated as a load, then it can be modified according to physical constraints, risk category or probabilistic arguments. This needs to be analysed very carefully because the fuel content is not truly a load, in what concerns structural analysis. The fuel load has to be converted into energy, which involves many other parameters such as building geometry, encapsulation, etc. This energy then needs to be transferred to the structure, which once again adds additional parameters. It is the energy transferred to the structure that represents the load. Thus, a brief clarification of these parameters will be provided here.

Table 1 : Various coefficients presented in Eurocode Annex E [11]

<table>
<tr><td colspan="3" rowspan="2">Fire activation risk factor due of size of the compartment</td><td colspan="6">Floor area (m^2)</td></tr>
<tr><td></td><td>25</td><td>250</td><td>2500</td><td>5000</td><td>10000</td></tr>
<tr><td colspan="3"></td><td>δ_{q1}</td><td>1.1</td><td>1.5</td><td>1.9</td><td>2.0</td><td>21.3</td></tr>
<tr><td colspan="3" rowspan="2">Fire activation risk factor due of occupancy type</td><td colspan="6">Examples of type of occupancies</td></tr>
<tr><td></td><td>museum</td><td>offices</td><td>engines factories</td><td>chemical factories</td><td>fireworks factories</td></tr>
<tr><td colspan="3"></td><td>δ_{q2}</td><td>0.78</td><td>1.0</td><td>1.22</td><td>1.44</td><td>1.66</td></tr>
<tr><td rowspan="11">Fire Fighting Measures</td><td colspan="2" rowspan="3">Automatic suppression system</td><td>δ_{n1}</td><td colspan="5">Automatic Water suppression system</td></tr>
<tr><td></td><td colspan="5">0.61</td></tr>
<tr><td>δ_{n2}</td><td colspan="5">Independent water supplies</td></tr>
<tr><td></td><td>0</td><td colspan="2">1</td><td colspan="2">2</td></tr>
<tr><td></td><td>1</td><td colspan="2">0.87</td><td colspan="2">0.7</td></tr>
<tr><td rowspan="4">Automatic Fire detection system</td><td rowspan="2">Automatic fire detection and alarm</td><td>δ_{n3}</td><td colspan="5">Heat detection</td></tr>
<tr><td></td><td colspan="5">0.87 or 0.73</td></tr>
<tr><td>δ_{n4}</td><td colspan="5">Smoke detection</td></tr>
<tr><td></td><td colspan="5">0.87 or 0.73</td></tr>
<tr><td>Automatic alarm transmission to fire brigade</td><td>δ_{n5}</td><td colspan="5">0.87</td></tr>
<tr><td rowspan="4">Manual Fire Suppression</td><td>Work Fire brigade</td><td>δ_{n6}</td><td colspan="5">0.61 or 0.78</td></tr>
<tr><td>Offsite Fire brigade</td><td>δ_{n7}</td><td colspan="5">0.61 or 0.78</td></tr>
<tr><td>Safe access route</td><td>δ_{n8}</td><td colspan="5">0.9 or 1 or 1.5</td></tr>
<tr><td>Fire Fighting devices</td><td>δ_{n9}</td><td colspan="5">1 or 1.5</td></tr>
</table>

		Smoke Exhaust system	δ_{n10}	1 or 1.5
Factors for protected fire loads		**Fire load with at least 10% of protected fire load**	ψ_i	1.0
		Fire load that cannot be ignited by unprotected fire load	ψ_i	0.0

The factor ψ_i corresponds to encapsulated combustible materials. This factor can eliminate combustible materials by assigning $\psi_i = 0$ in cases where encapsulation prevents the particular fuel load "i" from participating in a fire event. This is of critical importance in the case of timber structures, combustible insulation and composite panels, because the encapsulation can result in a very large reduction of fuel load. Encapsulation is a system by which a mechanical barrier provides thermal protection to the combustible material so that it will not attain ignition conditions. Being a mechanical barrier, the encapsulation needs to be carefully assessed to establish its reliability because mechanical failure of the encapsulation will result in an additional fuel load. The Eurocode does not provide any means for this assessment. In contrast, in the case of exposed mass timber, the timber in itself can result in self-extinction without encapsulation [21,22]. The Eurocode approach will assign to exposed timber $\psi_i = 1$ which will introduce the integrity of the structural timber as fuel load. In this case the characteristics of the material are essential to its favourable performance, nevertheless, the Eurocode approach will penalize timber by favouring encapsulation through the value of ψ_i. Thus, the treatment of ψ_i in Equation (3) requires attention that is product specific and goes beyond the information provided in the Eurocode.

The case of the δ_i is also of concern. The principle behind the modulation of a load by risk factors is associated with managing the probability of specific events. Thus, risk factors consider hazard categories and countermeasures to always deliver acceptable levels of risk.

Hazard categories establish contextual variables that change the level of risk, thus to appropriately manage risk compensation is necessary. This can come in the form of a risk factor. This is how a large and complex building located in a highly populated urban area might carry a higher risk-factor than a small and simple building in a remote area. A detailed assessment of the variables involved in the risk assessment is essential and generally these risk factors are mostly greater than unity. Table 1 shows two cases of hazard categories, compartment floor area and occupancy. In the case of occupancy, the nature of the activity defines its risk, thus the justification of the risk factor should be based on statistical data of historic events. While the Eurocode is not clear on the basis of this classification or quantification of the risk factors, the values are all conservative ($\delta_i > 1$) with the exception of art galleries, museums and swimming pools ($\delta_i = 0.78$). This will be discussed in more detail later.

The use of risk factors for trade-offs or compensation by means of alternative countermeasures is very complex. First, it is essential that the countermeasures provide true compensation, in other word, the inclusion of one countermeasure has to supplement the exclusion of another. Furthermore, issues of reliability need to be considered to guarantee that true compensation is attained. This applies whether the value of δ_i is greater or smaller than unity. In the case where $\delta_i > 1$, it is assumed that the structural protection works in conjunction with another countermeasure, thus the absence of this other countermeasure requires a $\delta_i > 1$. This is the case of safe access routes, firefighting devices and smoke exhaust systems (Table 1). In all the other cases, δ_i <1, a compensation is being claimed by which the added countermeasure substitutes for the role of structural fire protection.

A common and incorrect argument in favour of this approach is that this risk factors should be interpreted as a means to address a change in probability through countermeasures, where a value $\delta_i < 1$ is a means of moving through the statistically defined fuel load curve to an area of fuel load corresponding to a lower percentile, while a value of $\delta_i > 1$ is equivalent to moving towards an area with a higher percentile. With a reference percentile considered as an acceptable design value. This interpretation will be possible only if the fuel was the "fire load," but in this case, the "fire load" is the energy transferred to the structure. The relationship between fuel load and the thermal load applied to the structure depends on many variables, many of them having a much more significant impact than the amount of fuel. Nevertheless, by interpreting the risk factor in this way, the benefits of reducing the amount of fuel are translated linearly to the energy delivered to the structure. Equation (4) shows how the time to burnout, t_{BO}, is the solution to a highly non-linear equation that involves local burning rates, $\dot{m}''_f(x,y,t)$, and the total fuel load (M_f). In a similar manner, the fire load ($q''_e(x,y,z)$) is not only a complex function of the fire dynamics of the compartment but also is a spatially distributed function that is also a highly non-linear (Equation 5). As such, this interpretation is over simplistic and many times assigns a disproportionately beneficial impact of countermeasures on structural behaviour.

$$M_f = \iint_0^{A(x,y)} \int_0^{t_{BO}} \dot{m}''_f(x,y,t)\,dt\,dA(x,y) \tag{4}$$

$$q''_e(x,y,z) = \int_0^{t_{BO}} \dot{q}''(x,y,z,t)_e\,dt \tag{5}$$

Furthermore, it is necessary to understand the role that each countermeasure plays in the overall fire safety strategy. On this basis, it is possible to establish if structural performance can be truly compensated by the other countermeasures.

In the context of the fire safety strategy structural elements can be designed to five different performance levels, the most basic one is purely related to life safety where all structural elements need to fulfil their function until a point where their failure does not compromise the life safety of people, the next level of protection will be for structural elements to fulfil their life safety function but to allow for failure of structural elements only if progressive collapse can be arrested until burn-out of the fuel load, the third level is for structural elements to fulfil their life safety function but not to allow for failure of the structural elements until burn-out of the fuel load and the final level is for the structural element to fulfil their full function until burn-out of the fuel load. Low rise housing will fit in the first category, and thus require little or no structural fire performance, while super-tall buildings might require for structural performance to fulfil its full function until burn-out of the fuel.

Given the role assigned by the fire safety strategy to the structure, i.e. life safety function, then compensation has to be demonstrated if a reduction in structural performance is suggested, i.e. through reduction of the imposed fuel load by means of a risk factor. A proper compensation will be the introduction of a countermeasure that reduces the fire load (i.e. reduction of $q''_e(x,y,z)$). Instead, Table 1 shows that the fire risk factors can be grouped into two distinct forms of countermeasure, automatic water extinguishing systems and fire brigade intervention. In the case of automatic water extinguishing systems, both their presence and their reliability are granted a risk factor of less than unity ($\delta_{n1} = 0.61$ and $\delta_{n2} = 0.7 - 1.0$ respectively) and in the case of the fire brigades, it is assumed that early detection and notification is an enabler of more effective intervention, thus granting risk factors of less than unity ($\delta_{n3} = 0.87$ for heat alarms, $\delta_{n4} = 0.73$ for smoke alarms and $\delta_{n5} = 0.87$ for automatic alarm transmission to fire

brigades). In similar manner proximity and adequate access to fire brigades are also deemed to enhance their effectiveness, therefore, a risk factor of $\delta_{n6} = 0.61$ to 0.78 is assigned and $\delta_{n8} = 0.90$ for safe access routes. The specific quantitative values of these risk factors are not properly justified, but even if they were, the question of adequate compensation is not answered. In most jurisdictions the fire brigades are not considered part of the fire safety strategy but a contingency in case the fire safety strategy does not work correctly. Thus, the fire brigades are a redundancy and cannot compensate a primary function with the life safety function of structural integrity. In a similar manner a sprinkler is primarily a property protection measure intended to reduce the probability of a post-flashover fire. Structural performance is a life safety requirement that needs to be fulfilled to a standard defined by a fully developed fire, independent of the performance level targeted. Thus, the two measures act in parallel in the fire safety strategy and cannot be interchanged. Trading-off sprinklers for structural performance can therefore not be considered as adequate compensation to the life safety function of structural integrity. Despite the fact that neither fire brigade intervention or automatic water extinguishing systems are adequate compensations for structural performance, they are granted, as an ensemble, risk factors that can result in a massive reduction of the fuel load (>75%), which in turn is reflected directly in a significant reduction of the structural fire performance.

In the case of Table 1, it is clear that occupancy represents a hazard category and therefore it is consistent with the concept of risk factors. Unfortunately, from a quantitative perspective, the general categories presented in Table 1 are inconsistent with the nature of a fire safety strategy. The quantitative representation of a risk factor should emerge from a proper probabilistic risk assessment of the occupancy. While the risk assessment of most swimming pools will result in a very low fire hazard, however, the Summerland disaster demonstrated the opposite [23]. In contrast to occupancy, compartment size is much more difficult to argue as a hazard category. Compartment size alters the fire dynamics in a complex way, analysis methods become less robust as the compartment increases in size and experimental data is scarcer, therefore it can be argued that risk factors should increase with compartment size. Nevertheless, as for occupancies, only a proper risk assessment will enable quantification of the risk factor.

While the Eurocode provides some guidance that enables the quantification of the thermal load imposed by a fire on a structure, the methodologies proposed have fundamental misconceptions and weaknesses, thus this information needs to be treated with great caution.

4.3. NFPA 557

The methods presented in NFPA 557 [24] are deterministic but attempt to introduce risk based variables. NFPA 557 defines two types of fuel load; localized (concentration of combustible material at a location) and distributed (total fuel load throughout a compartment). According to NFPA, the design fuel load densities are determined by combining three factors namely; the statistical distribution of the fuel load within the building, fire initiation frequency (taken from the fire incident data), and the presence of effective and reliable fire protection features that contribute to fire control in the early stages of the fire. The combination of weighing (smaller items) and inventory survey (heavy items) methods is suggested in NFPA 557. While calculating the design fuel load, two types of fuel load are defined; fixed fuel load (combustible materials used as structural elements or as interior finish) and content fuel load (all movable and secure fire content in the compartment). NFPA 557 provides a procedure to determine the design fuel load for different occupancies. From survey, fuel load is calculated, and mean and standard deviation is specified for each type of building. And, further fuel load density is calculated based on risk objective (F) and the Gumbel distribution of fuel loads. A risk factor is obtained from the frequency of structurally significant fires (f_s) and risk performance criteria (R_s) of a structure (Equation 6), where R_s is defined by the appropriate code of a structure and its value must be lower than 10^{-6}/year for the collapse of a building. It is worth noting

that f_s is a function of floor area (A_f) as represented by Equation 7. Equation 7 implies that for larger floor area there is higher risk of significant fires, similar to Eurocode.

$$F = 1 - {}^{R_s}/_{f_s} \tag{6}$$

$$f_s = f_f A_f \tag{7}$$

where f_f is frequency of fires (obtained from the national statistical studies of fire incident data) which is defined for each occupancy for per million square meters per year. The average design fuel load density ($\bar{Q}_f$) is calculated from Equation 8.

$$\bar{Q}_f = \bar{Q}_{f,f} + \bar{Q}_{f,c} \tag{8}$$

where, $\bar{Q}_{f,f}$ and $\bar{Q}_{f,c}$ are the average of fixed fuel load density and average content fuel load density, respectively. The values of $\bar{Q}_{f,f}$ and $\bar{Q}_{f,c}$ are taken from the survey.

And, finally fuel load density (Q_f) can be calculated from equation 9.

$$Q_f = \bar{Q}_f + \frac{\sqrt{6}}{\pi}\sigma_f(0.577 + \ln(-\ln F)) \tag{9}$$

NFPA documents also provide the techniques of survey, however, like Eurocode, NFPA methods also require significant user effort along with the requirement of skilled and knowledgeable personnel to perform surveys to determine the fuel load density. NFPA documents, while simpler, follow a similar pattern to the Eurocode, therefore have the same type of guidance as well as suffering from very similar misconceptions. An advantage of the NFPA approach, as explained in Equation (9) is that in all circumstances$Q_f \geq \bar{Q}_f$, thus the approach to defining the fuel load is always conservative.

4.4. Probabilistic approach

Both of the above approaches (Eurocode and NFPA) do not fully account for the effect of floor area and usage of the compartment while calculating the design fuel load, they basically provide a single value of one type of occupancy that comes from the statistical data from extensive surveys. To improve the current practice Elhami-Khorasani et al. [25] proposed a probabilistic approach to determine the fuel load for office type occupancies that improves the calculation for fuel load density proposed by the codes and standards (Eurocode and NFPA 557). Using a Bayesian framework authors corrected the deterministic values presented in the codes by including the influence of the intensity of use (heavy use and light use) and the floor area of office buildings. The approach introduces the floor area as a multiplicative factor, a constant term which depends on the usage of the room and a selected value of fire load from the codes and standards. The constant terms for heavy and light use are determined from the surveys as represented in from Equation 10 (light use) and Equation 11 (heavy use). In their probabilistic model, they employed Culver's data, therefore this approach is limited to office buildings.

$$\ln(Q) + \theta_L = 6.951 \quad (10)$$

$$\ln(Q) + \theta_H = 8.252 \quad (11)$$

In Equations 10 and 11, Q is the deterministic value of the fuel load from codes and standards, and θ_L (for light use) and θ_H (for heavy use) are values determined from Culver's survey data.

4.5. AI approach

Recently a report has been published by NFPA research foundation about a novel method of estimating fuel load density using computer vision by Elhami-Khorasani et al. [26,27]. The proposed methodology employed recent developments in 5G technology, cloud storage, and artificial intelligence (AI). To facilitate the current survey methods, authors developed a method which consists of four major steps: (1) creation of a digital inventory (by taking the snapshots of all available material in a compartment, dimensions of contents and compartments), organizing the data (creation of a structured database), image matching (use of image recognition to get the information of each material) with available data, and quantifying the fuel load (by specifying the calorific value of each material). This method is quite sophisticated and relatively simple to apply to any kind of occupancy compared to surveys; however, it requires a large database. An application of this method can be found in [28]. Despite its advantages, it naturally has a limitation in discovering hidden of fixed combustibles that are unable to be captured in an image.

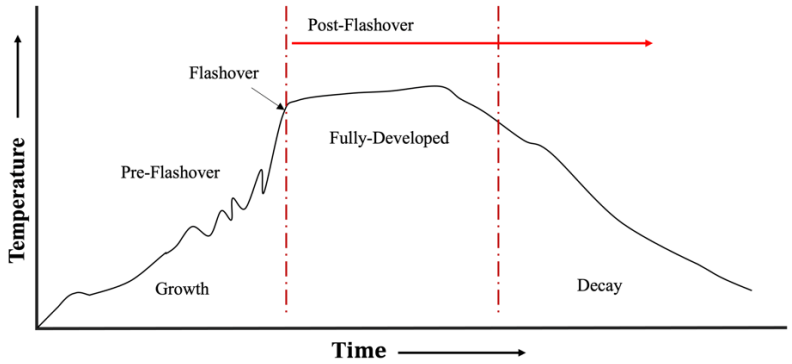

Figure 1: Stages of fire in a compartment

Figure 1. Stages of fire in a compartment

5. Development of Fire Models

When a fire starts in any compartment it undergoes a number of stages namely; ignition, growth, pre-flashover, fully developed, post flashover and decay as shown in Figure 1. These stages are defined as 'phases' by Magnusson and Thelandersson [29] that are subcategorised as ignition phase, flaming phase (when the fuel is burning and producing flames without any decay in combustion rate), and cooling phase (smouldering or decay in combustion rate). The correlations proposed for different stages of the fire are determined by applying 'conservation of energy', which is explained later in this section. Most of these

methods are based on the prediction of average temperatures by considering uniform gas temperatures in the compartment and do not consider local conditions.

For structural fire resistance, the focus has traditionally been on the post flashover stage of the fire, because the growth period was deemed as being of sufficiently low temperatures and short duration so that it had no impact on the structure. One of the earliest work to understand the structural response to fire, was performed by Kawagoe [4]. Using experimental results he introduced a physical basis to the standard temperature-time curve and established a concept of compartment fire and defined a link between ventilation (geometry), gas phase temperatures and burning rate, where mass burning rate depends on the size and shape of the vents (or openings) and deduced the expression below (Equation 12).

$$R = KA\sqrt{H} \quad (kg/s) \tag{12}$$

where R is the burning rate, A and H are the area and height of the openings in the compartment and K is a constant whose empirical value is proposed in various experimental and mathematical models [4,30,31]. It is worth noting that the validity of this correlation is restricted to the geometry of a compartment (size of the vent, aspect ratio, compartment size, etc) as assumptions are linked to the geometry.

The work of Kawagoe was followed by Thomas [5] who established engineering expressions that characterise the maximum temperature within a compartment. Thomas measured maximum temperatures averaged over the entirety of the compartment and presented a relationship of temperature with ventilation characteristics of a compartment (Figure 2). In Figure 2, *x*-axis represents the opening factor (or ventilation condition), where A_s is the surface area of the compartment. He explained this relationship in the form of regimes; Regime I, where enough soot is present and supply of oxygen is limited, and Regime II, where vents are big enough and soot concentration is lower, and combustion is independent of air supply. Harmathy [32–34] termed these regimes as ventilation controlled and fuel controlled, respectively. Thomas's work provides the worst-case time invariant temperature regime for the fire until fuel burnout. Nevertheless, the proposed temperature-opening factor relationship is applicable only for fully developed ventilation-controlled fire scenarios. Thomas did not propose a mechanism to calculate the heat transfer from the fire to the structure, although, this will be somehow a circular argument because, as described by Torero et al. [35] an assessment of the energy absorbed by the structure is part of the assumptions leading to the ventilation factor.

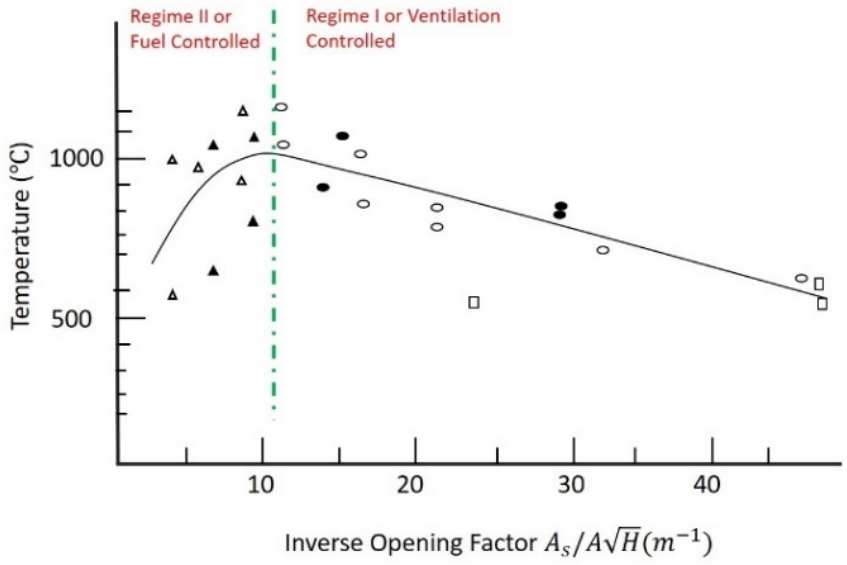

Figure 2: Classical curve for representing the relationship of temperature with ventilation factor.

Various methods to study the Thomas Regime I fire (ventilated controlled) can be found SFPE handbook [6] to predict gas-temperatures for both pre-flashover and post-flashover conditions. Most of these methods are applied for well-ventilated conditions only and correlation for the gas mass flow rate Kawagoe's expression is used.

Generally, fire models are used to calculate heat fluxes over structural surfaces as boundary conditions. Heat fluxes are determined using energy conservation. The presented form of the energy conservation equation (Equation 13), revisited by Torero et al [35], is used to develop most of the fire models.

$$\frac{dQ_{cv}}{dt} = \dot{Q}_{in} - \dot{Q}_{out} + \dot{Q} - \dot{Q}_w \tag{13}$$

where, Q_{cv} is the total enthalpy of the control volume, Q_{in} and Q_{out} are enthalpy entering with the reactants and enthalpy leaving with the products, respectively. Q_w represents heat losses to the surfaces of enclosures and Q is heat generation within the enclosure as shown in Figure 3. To calculate the heat fluxes on the surface, the major assumptions include that all oxygen entering the compartment is consumed during the combustion process, radiative losses through the openings are neglected, the temperatures for both gas phase and solid surface of the structure are assumed to be distributed uniformly. These assumptions are also necessary for the burning rate to be governed by the Kawagoe expression (Equation 12). Based on the above-mentioned simplifications, the heat transfer boundary condition at the surface can be expressed by Equation 14:

$$\dot{Q}_w = A_s h_t \left(T_{gas} - T_w\right) \tag{14}$$

Where h_t is the total heat transfer coefficient (including both radiative and convective terms) and A_s is the area of the surface over which flux is estimated. Equation 13, with all the appropriate simplifications, will provide the maximum temperature (T_{gas}) for Regime I of Thomas (full combustion). It is important to note

that Thomas did not use Equation 14 but substituted this equation by the data of Figure 2 and did not provide any method to estimate h_t.

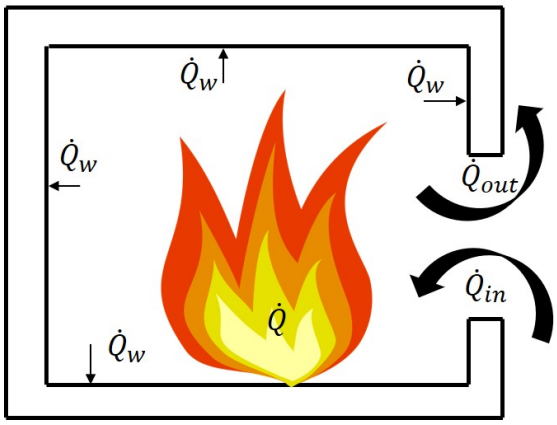

Figure 3: Representation of terms used in Energy balance in a compartment

Given that not all fires lead to flashover, but achieve steady-state conditions without reaching fully developed state, McCaffrey et al. [36] approximated the energy balance equation to predict pre-flashover conditions and calculate the gas temperature in the upper hot layer. They proposed a correlation (Equation 15) for the gas temperature rise (ΔT_g) in the hot upper layer. The upper layer was assumed to have a uniform temperature in a naturally ventilated compartment. The heat transfer coefficient (h_k) presented in Equation 15 depends on the thermal penetration time. The thermal penetration time is a characteristic time that establishes how far the solid phase is from reaching steady state conditions. When steady-state conditions are attained the temperature profile in the solid is assumed to attain a linear function and thus h_k becomes proportional to the conductivity of material. For transient conditions, the ratio between the penetration time and the characteristic time of burning serves to estimate h_k. As all other methods of this type, McCaffrey's method is completely based on experimental data, where the fuel was burnt near the centre of the room, so it can only be applied to similar conditions. Based on the assumptions, the correlation is only applicable where temperature does not reach more than 600°C (which is usually considered the inception of flashover conditions) and is capped at this value. Other researchers followed this work to improve the correlation for forced ventilation fires and provided additional empirical terms to modify McCaffrey's method. e.g. Foote et al. [37], Beyler et al. [38], Peatross and Beyler [39]. McCaffrey's correlation is as follows:

$$\Delta T_g = 6.85 \left(\frac{\dot{Q}^2}{A_T h_k A \sqrt{H}} \right) \tag{15}$$

where $\dot{Q}$ is the energy release rate of the fire and A_T is the total surface exposed to fire.

5.1. Extension of classical study

Two more simplified models are worth discussing in terms of measuring average temperature in a compartment, one proposed by Babrauskas [40] and another by Law [41].

5.1.1. Babrauskas correlation

Babrauskas [40] proposed a method to approximate post-flashover temperatures using several empirical factors and the concept of adiabatic flame temperature, as presented in Equation 16. He included five factors ($\theta_1, \theta_2, \theta_3, \theta_4, \ and\ \theta_5$) which were used with an empirical value of temperature (T*) obtained based on predicting stoichiometric conditions with no heat losses (adiabatic flame temperature). These factors vary between 0 and 1,and are determined from known parameters about the burning rate of fuel and its characteristics, losses to the wall, opening factors and efficiency of combustion (explained in detail in this section). The proposed expression simplifies the calculation; however, all unknowns need to be determined. He compared his results with the results obtained from a computer calculation (COMPF2) by employing the heat balance equation (Equation 13) in a compartment [42].

$$T_{gas} = T_\infty + (T^* - T_\infty).\theta_1.\theta_2.\theta_3.\theta_4.\theta_5 \qquad (16)$$

In the above expression (Equation 16), T_∞ and five $'\theta s'$represent the ambient temperature and efficiency factors, respectively that are discussed below. The author chose T^* values that fitted better with the adiabatic flame temperature obtained in a compartment, and lowered its value by assuming that no perfect stoichiometric condition is present in a compartment, which means there are some losses. Finally, he proposed an empirical value of 1725 C° for T^*. The paper does not provide a convincing reason for this choice.

θ_1 represents efficiency of the burning rate of a combustible in air against burning under stoichiometric conditions. θ_1 was calculated for both fuel-rich and fuel-lean regions incorporating equivalence ratio (ratio of actual burning rate with the burning rate at stoichiometric condition) in the expression. Equivalence ratio depends on the ventilation factor and burning rate, where burning rate was obtained from the empirical relationships for wood cribs and liquid (and thermoplastic) pool fire. It is worth noting that as burning rate varies with time and depends on chemical kinetics, therefore the expressions for θ_1 are valid only for wood and liquids (fuels having well established empirical expressions for burning rates) in a flashover condition.

θ_2 represents losses to the wall (or ceilings) under steady state conditions and depends on the ventilation factor ($A\sqrt{h}$), thickness (L) and area of the wall (A_w), and conductivity (k) of the materials of construction. As these values are known, the influence of two key variables ($\frac{A\sqrt{h}}{A_w}$ and L/k) on the losses (under steady state) were estimated over a wide range of these variables, and fitted to obtain an expression for θ_2. θ_3 represents the transient losses to the wall (or ceilings). By employing the Fourier number, the transient losses were plotted based on known variables ($\frac{A\sqrt{h}}{A_w}$ and $t/k\rho C_p$) as before (for θ_2) and an expression that fit the curve was proposed. Although wall effects were not modelled for lower value of time (t) i.e. initial stage, therefore the expression for θ_3 is valid for flashover conditions only.

θ_4 represents the influence of opening height on overall heat balance. The variation of radiation heat losses due to the height of the openings is plotted against numerical results, and an expression for θ_4 was deduced which depends on the height only. Finally, θ_5 represents the influence of combustion efficiency, which characterizes the degree of mixing of the fuel and air on the gas temperatures. An expression for θ_5 is deduced based on measured fires. This expression is limited to the types of fuel for which the combustion efficiency is known.

The author argued against accounting for types of fuel as it was found that among common fuels such as wood and hydrocarbon fuels the difference in the influence of the ratio of heat of combustion of the fuel to the mass of air and fuel composition is negligible. Furthermore, no significant influence of the wall and fire emissivities were found. However, it should be noted that in real fires, as discussed in section 4, different types of fuel would be available, therefore Babrauskas correlation would not be valid as complex kinetics may be involved. Also, as mentioned earlier, it is applicable for flashover conditions only, so the expression cannot be used for large open floor plan compartments, where radiation losses would be significant over a long period of the fire. Babrauskas [40] correlation provides only the average gas temperature reached inside the compartment by assuming similar conditions as those of Kawagoe and Thomas, therefore this method belongs to same category as those classical methods.

5.1.2. Law's empirical correlation

A notable extension and modification of Kawagoe and Thomas curve was introduced by Law [41]. Law proposed a correlation to calculate the maximum average gas temperature during the fully developed phase of fire. She evaluated – empirically – the average gas temperature (T_{gas}) in a compartment (fully developed fire) as shown in Equation 17. To obtain Equation 17, the author used the Thomas' curve (Figure 2) and used mathematical functions to fit the data (from mostly wood crib tests) obtained from many experiments conducted internationally [19].

$$T_{gas} = 6000\frac{(1 - e^{-0.1\varphi})}{\sqrt{\varphi}} \ (°C) \tag{17}$$

$$where, \qquad \varphi = \frac{A_T - A_0}{A_0\sqrt{H_0}} \ (m^{-0.5})$$

where A_T represents the total surface area of the enclosure (including windows) and φ represents the ratio of exposed area ($A_T - A$) to the opening factor. She explained the dip in the Thomas' curve from the function φ (inverse ventilation factor). When φ value is low (high ventilation) HRR would be high, however as the opening size is larger gas temperatures are lower because of higher heat losses. On the other hand, when φ is higher (low ventilation, regime I of Thomas curve), the heat losses are lower, however, heat release rate is also lower resulting in lower temperatures again. Maximum temperature was attained for $\varphi = 12$. Law further argued that when fuel load is lower, lower gas temperature would be obtained. Law modified the above expression (Equation 17) by including the effect of the fuel load (M) as expressed in Equation 18. The factor ψ (depends on the fuel load and geometry) was also deduced from the experimental data to fit the curves.

$$T_f = T_{gas}\left(1 - e^{-0.1\psi}\right) \ (°C) \tag{18}$$

$$where, \psi = \frac{M}{[A_0(A_T - A_0)]^{0.5}} \ \left({}^{kg}/_{m^2}\right)$$

Law further argued that structures are not only affected by gas temperatures alone but also by the duration of heating that must be quantified to estimate the fire resistance of a structure. It was the first time that the severity of duration of fire was introduced to Thomas's curve in terms of fuel load and compartment geometry. During fire if all the fuel is allowed to burn, the duration of fire can be expressed as Equation 19.

$$\tau = \frac{M}{R} \ (s) \tag{19}$$

where τ is the fire duration. R (rate of burning) depends on the opening factor (Equation 12). Consequently, at lower opening factors, duration of burning would be higher, which could result in more severe impact on the structure. Law also suggested that the duration of fully developed phase was about half of the total duration of fire, that begins when the fuel mass reduces to 80 percent of initial mass and ends when it reaches 30%. The average gas temperature during the fully developed stage is estimated by Equation 17 obtained by fitting curves to experimental data.

Like Thomas's expression, Law's correlation is also applicable to ventilation-controlled fires with a uniform temperature inside the compartment for a fully developed fire.

5.2. Parametric curve

In the early 70s, to overcome the limitation of standard fire curves, numerous curves were developed which represent the time-temperature relationship for a fully developed fire, and its dependency on the characteristics and quantity of fire load, and geometry of a compartment. One of the foremost investigations to determine the variation of temperature with time — including the cooling phase temperature — was conducted by Magnusson and Thelandersson [29]. They argued that temperature-time curves that are largely employed in structural engineering designs represent the fire duration well only in the flaming phase. Classical curves that are adopted widely do not provide any relationship between the fire load and the duration of fire, and physical explanation of the cooling phase is completely ignored (standard curve, Swedish Curves, ASTM E118, etc.). The calculation for flaming temperature does not take account of the combustion rate and the effects of openings on the temperatures even though the flaming phase depends on the opening factor over the duration of fire. The duration of fire (t) is defined as the duration of flaming phase and depends on the fire load (M) and opening factor (Equation 20).

$$t = MA_T/(25A\sqrt{H}) \tag{20}$$

The primary objective of their work was to find rational temperatures during the decay stage of fire that could be determined for different values of opening factor, fire load and structural material.

The Swedish curves represented the decay phase combustion gas temperatures as a linear decrease of temperature of 10°C / minute (an empirical value). This approach is presented in the Swedish Building Regulations (1967), as shown in Figure 4, and is similar to that proposed by Kawagoe [4]. No physical explanations were provided for the decay phase. Combustion during the decay phase is complex as only remnants of combustible materials are available and traditional ways of establishing heat release and burning rates no longer apply.

In classical studies, a fixed decay rate was usually selected arbitrarily, however, Kawagoe suggested that the decay rate depends on the duration of fire. From experimental observations, he proposed that a decay rate of 7°C / minute for a fire that lasts for more than one hour and 10°C/minute for a fire lasting less than an hour. While this could appear to be logical, given that fire duration equates to higher maximum

temperature for the solid surfaces, it is clear that this relates to heat transfer processes influenced by solid hot surfaces and is not a true representation of the gas phase temperature.

Magnusson and Thelandersson [29] observed that the decay rate depends on both the duration of fire and the opening factor (discussed later in this section). Once again, this observation seems to relate more to the solid surface temperature than to the gas phase. SFPE suggests that in the absence of adequate information, a decay rate of 7°C/minute can be selected for a fire lasting less than an hour [8]. Magnusson and Thelandersson [29] emphasised that the decay rate may influence the fire resistance period of the structural component therefore it is imperative to have a realistic temperature-time curve for the whole fire duration.

It is important to reiterate, that while details of these studies are not provided in the reports, the fact that all authors emphasise that the duration of the fire affects the decay rate, indicates that the decay rate is associated with solid phase cooling not gas phase cooling [1]. The gas phase cools rapidly, and the cooling rate is not affected by the fire duration, as when fuel burns out there will be no further heat generation. In contrast, solid phase heating and cooling are governed by the high thermal inertia of the construction materials, thus it will strongly depend on the heating duration [43]. Therefore, recommended decay phase temperatures need to be used with caution.

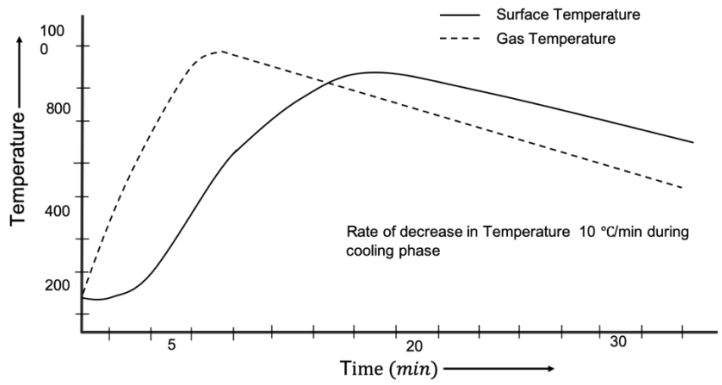

Figure 4: Swedish Curve for representing the relationship of temperature with time including cooling phase temperature for both solid and gas

The energy balance by Kawagoe and Sekine [44] and Odeen [45] is applicable during the flaming phase when rate of combustion is dependent on the mass flow rate of air exchange in the compartment. If the energy generated per unit time is known during fire development phase, energy balance can be deduced by determining the energy loss per unit time through conduction (to the walls and ceiling) and through convection and radiation at the ventilation openings. The assumptions to solve the heat balance includes; uniform temperature in the enclosure, uniform heat transfer coefficients, and one-dimensional heat flow through the bounding surfaces of the structure. However, Equation 12 (by Kawagoe) cannot be used to deduce the energy generation during the cooling phase as energy liberation is not governed by air supply in the cooling phase. Magnusson and Thelandersson [29] managed to deduce the compartment temperature throughout the heating and cooling phases by resolving each term in energy equation (Equation 13). For better understanding their method, following paragraphs demonstrate how each term was calculated.

Energy generation ($\dot{Q}$)

Magnusson and Thelandersson [29] used Equation 13 like Thomas (and revisited by Torero et al. [35]), explaining each term as illustrated in Figure 3. The energy generation within the enclosure ($\dot{Q}$) can be determined from the Equation 12 (during the flaming phase). To obtain the combustion rate with respect to time during the phase of fire development, authors used the results from experiments [4,45,46]. A computer program was developed to determine the compartment temperature over time based on an assumed combustion rate. The assumed time-temperature graph was varied until it agreed with the experimentally obtained temperatures over the whole flaming phase. The only criterion was to assume that the total energy liberated during the fire development process must be equal to the total energy of the fuel. It is worth noting that most of the experimental data used by Magnusson Thelandersson [29] involved wood cribs as fuel. The combustion rate variation with time was systematically plotted for various combination of opening factors and fuel load which made it possible to determine the curve showing the variation in combustion rate with time for a given fuel load or opening factor.

Heat loss at the openings

To calculate the heat loss at the openings ($\dot{Q}_{out} - \dot{Q}_{in}$) as a result of the exchange of hot gases with the cold air, Kawagoe and Sekine [44] used Bernoulli's equation to predict the quantity of outgoing gases and incoming air in the compartment as a function of temperature and neutral layer position (where the internal pressure in the compartment is equal to the external pressure as represented in Figure 5). Ahlquist and Thelandersson [47] deduced the position of the neutral layer as a function of the combustion rate (which varies from 0 to its maximum value) and temperature, which again depends on the opening factor.

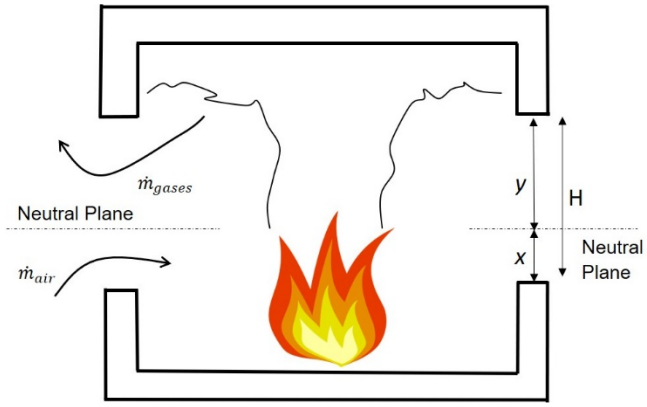

Figure 5: Gas flow and neural layer representation at an opening in a compartment

Assuming that the mass flow rate of the incoming air is equal to the mass flow rate of consumed gases during combustion, Kawagoe and Sekine determined the position of the neutral layer. If the quantity of the air consumed per unit weight is known, maximum combustion rate (R_{max}) can be determined. From the dimension of the openings and position of the neutral zone, the variation in the velocities can be determined, and the mass flow rate of outgoing ($\dot{m}_{out}$) and incoming air ($\dot{m}_{in}$) can be calculated as shown in equations 21 and 22.

$$\dot{m}_{out} = \frac{2}{3}\mu W (y)^{3/2} \sqrt{2g\rho_g(\rho_a - \rho_g)} \qquad (21)$$

$$\dot{m}_{in} = \frac{2}{3}\mu W(x)^{3/2}\sqrt{2g\rho_a(\rho_a - \rho_g)} \quad (22)$$

where μ is the coefficient of contraction of the opening, W is the width of the opening, and y and x are the vertical distances from the neutral layer to top and bottom of the opening, respectively. ρ_a and ρ_g are the density of the outside air and the hot gases, respectively.

Mass flow rate can also be determined by the maximum rate of combustion (Equation 12) in the form of equations 23 and 24.

$$\dot{m}_{out} = R_{max}\, G_0\, \rho_a \quad (23)$$

$$\dot{m}_{in} = R_{max}\, L\, \rho_a \quad (24)$$

where G_0 and L (measured in Nm^3/kg) are the volume of gases and air produced and consumed by the combustion of 1 kg of fuel, respectively.

It was found that R_{max} depends on the temperature difference between the hot gases and the fresh air (Equation 25). $\kappa(\Delta T)$ is a temperature dependent coefficient, calculated for wood and alcohol in [4]. It is nearly constant during the flaming phase where temperatures are assumed to be uniform in the fire compartment.

$$R_{max} = \kappa(\Delta T)A\sqrt{H} \quad (25)$$

$$\Delta T = T_g - T_a$$

where T_g and T_a are the temperature of the hot gases and fresh air, respectively. The expressions above hold true for the flaming phase only, where all air entering the compartment is assumed to be consumed and the combustion rate is constant. However, to calculate the combustion rate (R) for the whole process a coefficient 'a' is introduced to account for the proportion of oxygen in the outgoing gases (Equation 26). If the outgoing gases contain only air and no combustion products, 'a' is equal to zero, however, if outgoing gases contains combustion product only, 'a' is equal to 1.

$$R = a \times 330 \times (\Delta T) \times A\sqrt{H}\ \ (kg/h) \quad (26)$$

By assigning the value of R in Equations 21 to 24, a relationship between combustion products and air mixture proportion (a) and neutral zone location (y/H) is obtained (Equation 27)

$$\left(\frac{y}{H}\right)^{3/2} \times \rho_g(\rho_a - \rho_g) - \left(1 - \frac{y}{H}\right)^{3/2} = \frac{(G_o - L) \times \rho_a \times 330a}{\frac{2}{3}\mu \times \sqrt{2g}} \quad (27)$$

The heat loss from the openings can also be written in terms of specific heat of outgoing gases (C_p) as Equation 28.

$$\dot{Q}_{out} - \dot{Q}_{in} = \dot{m}_{out} \times C_p \times \Delta T / \rho_a \tag{28}$$

By substituting the values of mass flow rate of the outgoing gases, heat loss can be expressed as Equation 29.

$$\dot{Q}_{out} - \dot{Q}_{in} = \vartheta(\Delta T) \times C_p \times \Delta T \times A\sqrt{H} \tag{29}$$

where $\vartheta(\Delta T)$ is a factor that depends on the height of neural layer and temperature difference and can be expressed as:

$$\vartheta(\Delta T) = \frac{2}{3}\mu \times \sqrt{2g}\,\frac{\sqrt{\frac{\Delta T}{273}}}{1+\frac{\Delta T}{273}}\left(\frac{y}{H}\right)^{3/2} \tag{30}$$

For any given value of $\frac{y}{H}$, μ, G_0, and L authors plotted the variation of $\vartheta(\Delta T)$ for a number of values of 'a' and ΔT and found a relationship between ϑ and 'a'. Finally, if 'a' is known heat loss to the opening can be determined, and 'a' can be obtained from the combustion rate (determined by regression using the experimental data). In the calculation, it was also assumed that G_0 and L are constant throughout the whole process. As all experiments were conducted by using wood cribs, therefore the process explained above is limited to such.

Heat loss at boundaries ($\dot{Q}_w$)

To calculate the heat losses at all boundaries (walls, ceiling, and floor) of the compartment, represented by $\dot{Q}_w$, the general equation of non-steady conduction (Equation 28) was solved numerically.

$$C\rho\frac{\partial T}{\partial t} = \frac{\partial}{\partial x}\left(K\frac{\partial T}{\partial x}\right) \tag{31}$$

where, C is the specific heat of wall material, ρ is the density of the wall material and K is thermal conductivity.

Equation 31 was treated as an ordinary differential problem and solved by applying a modified version of the Runge-Kutta method [48]. The wall layer is divided into 'n' number of layers of variable thickness and temperature variations for small time intervals were calculated by invoking heat balance (Equation 13) for each layer. The resultant emissivity (including both from flames and surface) was approximated by considering two parallel surfaces for the radiation between the flame and the exposed surface. The radiation losses at the opening ($\dot{Q}_R$) were considered fixed throughout the whole process of fire development. Having all terms of the heat balance, gas temperatures can be obtained from the numerical treatment of the ordinary differential equations, that can be used to determine losses to the wall (Equation 32). Finally, the transient gas temperatures can be plotted for the whole process.

$$\dot{Q}_w = A_t h(T_g - T_1) \quad (32)$$

where h is the coefficient of heat transfer on the internal surface including both convective and radiative heat transfer coefficients. A_t is the area of the exposed surface, and T_g and T_1 are the gas and surface temperatures.

Based on the assumptions used, this model is applicable to fully developed ventilation controlled fires only, where temperatures are uniformly distributed over the surfaces of the structure similar to Thomas's study. Additionally, structural elements are fully engulfed in the fire so that gas temperatures can be assumed as radiative temperatures and emissivity of soot or gas can be approximated. These curves have been widely adopted and various parametric studies were performed, such as by Pettersson [49] who developed a number of time-temperature curves, currently referred to as the parametric fire curves.

Pettersson [49] extended the work of Magnusson and Thelandersson [29] and develop parametric temperature-time curves. Using the energy balance equation, gas-temperatures (T_{gas}) were calculated. He argued that standard temperature-time curves do not account for a number of important features that must be considered to achieve a rational design of structures, e.g. quantity and type of combustible material, fuel distribution in the compartment and geometry of the compartment. Like Magnusson and Thelandersson [29], he also argued that the rate of combustion (R_m) calculated using the Kawagoe's correlation (Equation 12) is valid for ventilation controlled fires (applicable during flaming phase only), however this correlation does not hold for fuel controlled combustion (Regime II), which theoretically depends on various other factors such as type of fuel load, the manner in which combustibles are stored (distributed), etc., which makes it difficult to derive an analytical solution for combustion rate.

The opening factor and rate of combustion relationship as shown in Figure 6 is similar to the Thomas's curve (Figure 2). The right side of the curve can be considered as Regime II of Thomas. Higher values of mean rate of combustion are obtained for larger fire load.

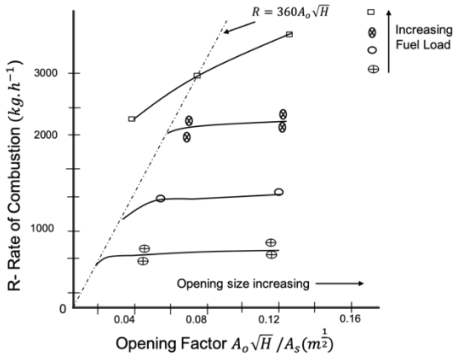

Figure 6 : Relationship of rate of combustion with opening factor for different fuel load (redrawn from [29,49])

Based on same assumptions and simplifications as Magnusson and Thelandersson [29], Pettersson [49] developed parametric curves for a number of ventilation factors and different types of the compartments (based on construction material such as concrete, steel, composite, etc), for fire protected and bare structural steel members. At first, parametric curves were produced for one type of material for a standard compartment for various opening factors (using modified version of the method of Magnusson and

Thelandersson [29]). For other types of construction, an equivalent factor determined from experimental data was used for the fuel load and opening factor. These curves are widely used in structural design for fire resistance.

The parametric curves from Magnusson and Thelandersson [29] and Pettersson [20] also provide uniform temperatures in the fire compartment and are applicable primarily for ventilation controlled scenarios.

5.3. Standard fire curves

The curves and correlations discussed in the previous section mainly provide average gas temperatures for fully developed or post-flashover fires, which can be used to determine the thermal boundary conditions for structural analysis. However, standard Temperature *vs* Time curves are much more commonly used in structural engineering problems even though they do not represent a real fire and have other significant limitations. In a review article, Gales et al. [50] provide a historic narrative of the standard-time temperature curves. A brief introduction is provided in this section for the standard, nominal and parametric curves, and summarised in Table 2 along with the limitations and assumptions associated with each.

Standard temperature-time curves are widely used by structural engineers because of their simplicity. These curves represent a continuously increasing temperature with time without any decay or cooling phase. The cooling phase has consistently been demonstrated to be important in terms of structural strength. For example, Hertz performed an experimental study for a fully developed fire scenario and tested the strength concrete column, it was found that load bearing capacity of column decreased by half during flaming phase and other half in cooling phase [51].

A standard set of curves were published in Eurocode I [11] and presented as nominal Temperature-time curves and then Equations 36 to 38 are used to calculate the heat fluxes on the surfaces of structural components. The calculations use a prescribed value of convective heat transfer coefficient ($h_{convective}$) e.g. 25W/m^{2}K for the standard fire curve (ISO834) and 50W/m^{2}K for the hydrocarbon curve. These prescribed values are likely to deliver inaccurate results as convective heat transfer coefficient varies with length scale and velocity of the hot gases, therefore its value depends on structural component (beams, trusses or columns) size and severity of fire. For thin structural elements such as trusses or web openings of cellular steel beams, the convective heat transfer coefficient could be significantly higher than the prescribed values [43].

These nominal fire curves also assume uniform gas temperature inside a compartment, and structural members are considered fully engulfed in the fire therefore unit emissivity and unit configuration factor is recommended in the absence of better data. These assumptions are reasonable for fire-scenarios with no radiation losses and a compartment full of soot.

$$\dot{q}_{net} = \dot{q}_{convective} + \dot{q}_{radiative} \tag{36}$$

$$\dot{q}_{convective} = h_{convective}\left(T_{gas} - T_{surface}\right) \tag{37}$$

$$\dot{q}_{radiative} = \varphi . \varepsilon_{surface} . \varepsilon_{fire} . \sigma\left(T_{radiation}^4 - T_{surface}^4\right) \tag{38}$$

Equation 38 represents the radiative heat fluxes over the structural surfaces, where φ is the configuration factor and ε_{fire} and $\varepsilon_{surface}$ are the emissivities of fire and surface, respectively. The radiative fluxes are simplified by assuming the emissivity of fire as one (all radiation energy reaches the surfaces), and gas temperatures are taken as radiation temperatures by assuming thermal equilibrium of the radiation field in the gas phase which further represents that there is no radiation exchange between soot and gas which is theoretically inaccurate and fails to account for the physics of radiation exchange. The greatest shortcoming of the standard fire curves is that they have no connection to the real fuel load, nature of the materials, geometry of the compartment and its ventilation characteristics, all of which have a significant influence on the compartment temperatures and heat transfer rates.

5.4. Eurocode 1

In the European code for structural fires, a number of correlations are presented to calculate the gas temperature and heat fluxes over structural surfaces. These mathematical correlations and their limitations and assumptions are presented in Table 2. Standard curves or nominal curves are already described in the previous section. Eurocode I [11] provides parametric curves which define gas temperatures over time during the heating and cooling phases. These temperatures can be used to calculate heat fluxes using the Equations 36-38. Eurocode parametric curves are limited to smaller compartments of 500 m^2 floor area or less. This can be severely limiting in modern construction, especially industrial and business occupancies which usually have much larger floor areas.

Franssen [52] conducted dozens of experiments and found a weak relationship between the steel temperatures obtained from parametric curves and the measured temperatures during experiments. He recommended modifications in Eurocode I for walls of different thickness and weight, and insulation characteristics of wall materials. The modified model is able to provide more accurate compartment temperatures as a result of better accounting for the loss of heat at the compartment boundaries.

5.5. Localized fire model

Most structural fire resistance is designed to resist a high temperature over a specified duration of time based on the standard or parametric fire models discussed earlier, which imply an assumption of uniform temperature in the whole compartment as a result of fully developed fire. Where a compartment fire assumption cannot be used, either because of the size or characteristics of a compartment or because of the nature of a fire, such as a car fire in a parking structure or stacked storage items in a warehouse, localised fire models have been traditionally used. One of the earliest experimentally derived correlations for a localised fire was proposed by Hasemi et al. [53] in Japan. Hasemi's [54–56] localised fire model is presented in Eurocode I for two cases, when the flames impinge directly on the ceiling; and when the flames do not reach the ceiling.

The results from Hasemi's experiments were plotted and generalized using a correlation based on the parameters influencing the temperatures within the compartment. Gas temperatures (T_Z) at any location (z) along the localised fire plume can be calculated using the correlation presented in Equation 39, for the case when the flames do not reach the ceiling or the height of the flame is less than the height of the compartment.

$$T_Z = 20 + 0.25{Q_c}^{2/3}(z - z_0)^{-5/3} \leq 900 \quad (39)$$

Table 2: Summary of some notable fire models

Models		Curve/Features	Assumption	Limitation
Nominal Temperature –Time curves (Eurocode I) [11]	ISO834 Hydrocarbon ASTM E118	-Simplest method -widely used in structural designing -gas temperatures are used to calculate the heat fluxes over the surfaces	-uniform temperature - radiative temperatures are taken as gas temperature -configuration factor as one -fixed convective heat transfer coefficient values	-no representation of cooling phase of the fire - no link with fuel load or ventilation or geometry of compartment -applicable where optical length can be very small to utilise the local radiation effect
Magnusson and Thelandersson [29]		-represents cooling phase temperature -applicable for different kinds of structural material and fuel load -expression for horizontal and vertical openings	-complete combustion, where all air and fuel are consumed -uniformly distributed temperature -products of combustion gases and air have same specific heat and their volume remains constant	-applicable for only ventilation-controlled fire -only for fully developed fire and room full of soot
Pettersson [49]		-extended study of Magnusson -parametric curves are provided for different opening factors	Same as of Magnusson	Same as of Magnusson
Babrauskas [40]		-provided theoretical correlation -various factors are quantified, like combustion, ventilation opening	-empirical constant for highest temperature reached during combustion -for flashover condition and temperature is uniformed throughout the compartment	-ventilated controlled fire scenarios
Law [41]		- provided the correlation for the duration of fire -expression for fire load was also introduced	-Uniform temperatures -fully developed fire	-ventilated controlled fire scenarios
Eurocode I [11]	Parametric Fire	-correlation of both heating phase and cooling phases are presented	-Fuel is completely burnout	-applicable for area below 500Sq. m - ventilated controlled fire scenarios
	Localised Fire	-expression for two fire scenarios is given (Flame reaches to the ceiling and where flame does not reach to the ceiling	-surface temperature is considered as gas temperature - a number of empirical values are present in the correlations	-applicable where heat release rate is below 50 MW -loss of radiation was not presented -radiation from the soot was not depicted in calculation

In Equation 39 $Q_c(\mathrm{W})$ is the convective component of the heat release rate, which was approximated to be 80% of the total heat release rate (Q). z_0 is the virtual origin of the plume central axis, that can be determined by the equivalent diameter D of the fire source and total heat release rate (Equation 40).

$$z_0 = -1.02D + 0.00524Q^{2/5} \tag{40}$$

When flames impinge on the ceiling, Hasemi provided the following correlations from testing various configurations and presented the relationship with the diameter of fire and horizontal length of the flame. The empirical correlations to calculate the heat fluxes at any location (r) on the ceiling are presented with respect to the non-dimensional ratio (y): distance of the location (r) from the virtual location to the total length of the flame (Equation 41).

$$y = \frac{r + H + z'}{L_H + H + z'} \tag{41}$$

where z' is the vertical position of the virtual source with respect to the burner (virtual point of fire source) and determined by using non-dimensional heat release rate (Q^*) (calculated using Froude number). L_H is the horizontal length of the fire.

$$Q^* = \frac{Q}{1.11 \times 10^6 D^{5/2}} \tag{42}$$

$$z' = 2.4D\left(Q^{*2/5} - Q^{*2/3}\right) \qquad for\ Q^* \leq 1$$

$$z' = 2.4D\left(1 - Q^{*2/5}\right) \qquad for\ Q^* > 1$$

Using the above expressions, Franssen et al. [57], presented the heat flux (q') received at the ceiling, which were adopted in Eurocode 1 (Equation 43).

$$q' = 100\ (KW) \qquad for\ \ y \leq 0.3$$

$$q' = 136.3 - 121y\ \ (KW) \quad for\ 0.3 \leq y \leq 1 \tag{43}$$

$$q' = 15y^{-3.7}\ \ (KW) \quad for\ y > 1$$

As localised fire models are used for larger floor areas, Dai et al. [58,59], used Hasemi's localised fire model to propose a travelling fire model (discussed in section 6.3). Hasemi's model does not provide any information for radiation losses from the flame. The effect of radiative fluxes on structural surfaces would be influenced by the products of combustion i.e. water and CO_2, therefore the radiation reaching the surface depends on their emissivity as well and not just soot emissivity. These limitations make Hasemi's localised fire model highly conservative and also less scientifically robust as energy balance is not accounted for. Furthermore, as the correlations are based on small scale experiments, Hasemi's models are limited to a fire of diameter 10m and maximum heat release rate of 50MW.

6. Performance-based Engineering for Structural Fires

The evolution of fire models to characterise temperatures in fire enclosures include probabilistic (or stochastic) and deterministic models [6,60]. Probabilistic models do not explicitly use physics and chemical kinetics involved in fire development, instead rely solely on statistics based on data from extensive collections of experiments and actual fire incidents. On the contrary, deterministic fire models represent the fire processes mathematically based on physics and chemistry to analyse the dynamics of fire. With ever-increasing capability of computational hardware and software, and growth in the fundamental knowledge and understanding of fire processes, a large number of fire models have been introduced in the past five decades. Zone models and field-models are continuously being developed to provide more realistic approaches to determine temperatures inside an enclosure during a fire and the corresponding structural surface temperatures. Since the collapse of WTC Towers, research using field models to understand real fire scenarios in buildings and infrastructure has accelerated [61,62]. Some notable work to accomplish performance-based design (PBD) for travelling fire (discussed in section 6.2) has been carried out by researchers, where a few methods are suggested to quantify the temperatures in the large compartments in modern open-plan buildings.

6.1. Zone Models

The most common and the simplistic computer models are zone models, where generally compartment is divided in two gas zones i.e. upper (hot) zone and lower (relatively cooler) zone as a result of thermal stratification. Zone models are able to predict the macroscopic features (temperature in each zone, height of each layer etc.) of the enclosure. Conservation equation for mass, energy and species are invoked for each zone (upper and lower gas zones). However, conservation of momentum is not explicitly solved hence the transport time of species and flames is not accounted for in zone models. The upper layer (ceiling jet) is instantly produced, however in reality the formation of ceiling jet is transient. A detailed survey of zone models can be found in [63] and [64]. Each zone model includes sub-models [6] that describe the various combustion processes and transport phenomenon. These sub-models are specific to the problem such as; entrainment model which is critical to representing a developing fire [65], vent flow models which is crucial when a number of compartments are linked.

Cadorin and Franssen [66] developed a zone model (OZone) to determine the thermal boundary conditions for structural analysis in FEM (SAFIR). Once flashover (fully developed fire) is achieved, the two-zone model changes to a one-zone model and the time-temperature (or heat flux) history can be obtained for use in SAFIR. The transition from the two-zone model to one-zone model is deemed to occur once a pre-set criterion for flashover is reached (e.g. temperature in the upper layer reaches the pre-set flashover temperature and/or height of the interface reduces to lower than 20 percent of total height). Zone models also provide uniform temperatures in a post-flashover fire compartment to be used as structural boundary conditions.

Although zone models are simpler, faster, and computationally economical, there is a trade-off against accuracy. The properties of the upper and lower layers are assumed to be spatially uniform and both layers are assumed to be homogenous, which usually results in highly conservative estimates of temperature. Generally, convective heat transfer varies along the length (both vertically and horizontally) as convection varies with the local boundary temperature rather than bulk temperature and given that velocities are also assumed to be constant in both layers (momentum equation is not used), therefore the convective heat transfer is not explicitly computed in zone models. Radiative heat transfer to the surface is also calculated by assuming a uniform gas layer and the contribution from the flame is dependent on empirical data and in

most zone models usually a rectangular compartment is considered to calculate the configuration factor. Therefore, the results for large open-plan floor fires where a travelling fire might be observed (as in WTC), zone models are not practical. Forney [67] presented a sub-model to calculate the radiative heat flux for N walls assuming a rectangular compartment. This model is used in CFAST zone model developed by NIST.

6.2. Travelling fire models

Floor plans of modern office buildings are significantly larger with continuous open spaces compared to the enclosures where fire tests had been originally conducted to derive traditional post-flashover compartment fire models. The assumptions of uniform temperatures and homogeneous smoke layers in traditional compartment fire models break down for real fire scenarios that may play out in large open plan modern spaces [68]. Often fires are observed to travel across floor plates in large spaces, and also vertically between floors, as seen in the WTC Towers in 2001, the Madrid Windsor Tower fire in 2005, the Faculty of Architecture building fire in TU Delft in 2008, the Grenfell tower fire in London in 2017, and Plasco Building in Tehran in 2017. Such fires are increasingly being referred to as a "travelling fire", starting locally and spreading across entire floor plates while becoming extinct at locations of origin as the fuel burns out [69]. Such behaviour results in highly non-uniform temperature distributions across the floor plates as found in the investigation of the WTC incident conducted by NIST [62], where CFD simulations showed fires exhibiting a "travelling" behaviour over the floor plate. Data from various experiments of relatively larger compartments showed that the condition of relatively uniform temperature does not hold well [69,70]. Despite clear findings like this, most modern buildings continue to rely on traditional compartment fire models for structural designs (based on the assumption of uniform temperatures within a compartment) regardless the size or geometry of the compartment. In a survey conducted by Jonsodottir and Rein [71] in a modern building (Informatics Forum at the University of Edinburgh), it was found that around 92% of the total volume of the building was out of range of the Eurocode limit for use of its parametric fire model [11]. Therefore, it is important to understand the fire dynamics of such fire behaviour and propose new methods to quantify the temperature evolution over time in modern buildings with large open plan floor spaces. Over the last two decades, several experimental studies have been performed to observe both the structural response and the fire dynamics within large compartments [72–74]. There have also been a few attempts to characterise travelling fires to enable performance based engineering of structures for fire resistance. Three of the most notable idealisations of travelling fires are discussed in this section.

6.2.1. Clifton's model

Clifton suggested one of the earliest models to account for the "travelling" effect of a fire [75]. He divided a compartment in a number of "design areas" referred to as a "firecell." At a particular time, each firecell could be under one of the four conditions i.e. fire, preheating, smoke logged or burnt out. A firecell that is burning may preheat and eventually ignite neighbouring firecells and then burn out resulting in the conditions of all the cells of the compartment changing from one condition to another. The Eurocode parametric curves are used to determine the temperatures of the burning firecells, and fixed temperatures are assigned to preheating and burnt out firecells, initially between 200 and 675°C, but changed to 400 – 800 °C in a later version of their method [76]. The size of the firecell was set according to the fuel load density in the first version of this model [75], however it was changed to 50m^2 for all fuel loads in the modified version. The fire spread rate was set as 1m/s for well ventilated conditions and 0.5m/s for ventilation limited scenarios which were based on Kirby's experiments [72]. While this approach is relatively crude and simple, however, it represented a step in the right direction towards acknowledging the real fire dynamics in large open plan compartments found commonly in modern office buildings. Clifton's model also does not explicitly account for energy conservation and ventilation conditions that may vary

considerably during the fire. Although parametric curves usually represent a ventilation controlled fire (discussed in previous sections),it is highly unlikely to have ventilation controlled fires in large enclosures [77], as fire spread is usually controlled by fuel load. Majdalani et al. [77] argued that classical ways of calculating the burning rate for ventilation controlled fires (Regime 1) are not justifiable in travelling fire scenarios.

6.2.2. Rein's model

Rein et al. [78] proposed a novel methodology to deduce temperature evolution over time in a compartment for travelling fire scenarios. Unlike Clifton's model, the fire compartment is divided into two regions based on the thermal conditions i.e. near field and far field, where near field is the region where flames directly impinge on the structural components, and far field are the regions where only a hot smoke layer is present and these regions are remote from the flaming region (Figure 7). The burning region "travels" over the floor plate of the compartment. A large range of fires, from fire covering a relatively small area to a whole compartment fire may be assumed as the possible fire scenarios. Fire size is decided by the specific area as a percentage of the total floor area. They proposed a family of fires covering 1% to 100% of the floor area, where 100% represents the conventional whole compartment post-flashover fire. Before proposing the analytical method, CFD was used as fire model [78]. However, in subsequent study, to ach 6ieve an analytical expression for the travelling fire, it was assumed that the fire load is uniformly distributed across the fire path where a fire may burn over a specific fire area (A_N) with a constant heat release rate per unit area ($\dot{Q}'$). The total burning time (t_f) (Equation 44) over the fire area is calculated on the basis of the fuel load per unit area (M).

$$t_f = \frac{M}{\dot{Q}'} \tag{44}$$

From the Equation 44, it is clear that time of burning is independent of the floor area but depends on the fuel load and HRR, and the values for both fuel load and HRR are taken from standards and codes [11]. Therefore, the time of burning would be same for any *fire area*. Eventually, the *total burning time* of the fire in the compartment would be inversely propositional to the *fire area* e.g. for smaller *fire area* the *total burning time* would be higher. As the design fire area moves across the floor plates and near field changes with each burning time of fire area and left behind the burnt out area that is now in cooling stage however considered as far-field as shown in Figure 7. So, fire spread rate (s) is determined by the time of fire and the length of the fire (L_f) area across the fire path (as it was assumed that all width of the fire is in burning stage in a specific fire area) as represented in Equation 45.

$$s = \frac{L_f}{t_f} \tag{45}$$

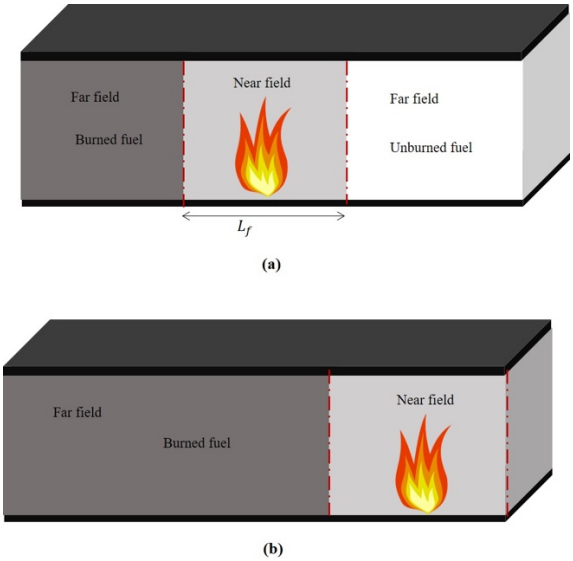

Figure 7: Travelling fire representing near and far field

They calculated the temperature fields in both regions separately. In the near-field (burning zone) which is dominated by the fire, temperatures are dependent on flame temperatures which are assumed to be uniform and in the range of 800-1200 °C (based on the fuel load), however, in original version of this proposed methodology it was conservatively fixed to 1200 °C [68]. Temperatures in the far-field depend on the rate of heat release and inversely with distance from the flame Structural components in the far field are assumed to be engulfed by the layer of smoke and hot gases below the ceiling. To calculate the far-field (hot-layer) temperatures authors used Alpert's correlation [79] (Equation 46) which represents the ceiling jet temperatures and provides peak temperatures (T_{max}) in a radial direction,

$$T_{max} - T_{\infty} = 5.38 \frac{(\dot{Q}/r)^{2/3}}{H} \tag{46}$$

where in Equation 46, T_{∞} represents the ambient temperature and $\dot{Q}$, r and H represent total heat release rate, radial distance from the flame and the height of the ceiling, respectively. It is worth noting that Alpert's correlation is meant for short distances [79] as the primary objective of Alpert's study was to predict the response time of detectors and sprinklers during the early stages of fire, not for large fires considered in Rein's model. Radiation losses were not explicitly included in Rein's model (following Alpert) with the major contribution to heat transfer to structural components near the ceiling was from convection. Furthermore, Rein's model does not provide direction of "travel" which increases the uncertainties in the model as fire initiation (ignition location) and direction cannot be known a priori; it does not account for the heat balance and used the fixed temperatures in the near field; and it assumes uniform fuel distribution along the path of travel.

6.2.3. ETFM model

Dai et al. [58,80] developed another approach for idealising travelling fires, called the extended travelling fire method (ETFM). Unlike Rein's model, ETFM calculates heat fluxes in the near-field region using Hasemi's localized fire model (as discussed in section 5.5) and a zone model (discussed in section 6.1) to deduce the heat fluxes in the far field. ETFM incorporates more of the fire dynamics of a travelling fire

behaviour in a large compartment, as the zone model accounts for both mass and energy conservation between the hot and cold zones. However, as Hasemi's model does not account for a smoke layer, radiative and convective heat fluxes from both models (Hasemi's localised fire model and the Zone model) are superimposed in the overlap zone heat fluxes in the near field are likely to be conservative. Essentially Dai et al. provide a generalized framework where any localized fire model can be used for calculating the near field temperature and any suitable zone model for the far field temperature. The key parameters required to define the Hasemi's model are; location of the fire, fire diameter, and heat release rate. From earlier discussion it is already clear that all these values change with time over the course of fire travel within the compartment. As discussed in section 6.1, zone models provide temperatures in the smoke layer and smoke layer interface height by solving the ODEs (mass and energy equations). It is important to know how the total heat release rate is calculated and the travelling fire speed for the localized fire model. The total heat release rate ($\dot{Q}$) is calculated using the expression presented in Eurocode 1 (Equation 47).

$$\dot{Q} = HRR_f \times A_f \tag{47}$$

where HRR_f is the maximum heat release rate per unit area (MW/m^2) of the fuel and A_f represents the burning area. HRR_f varies for occupancies as stated in Eurocode 1 and would depend on the fuel load. In the ETFM model, it is assumed that a fixed burning area (A_f) travels over the floor plate in a predefined trajectory and fuel is uniformly distributed over the floor.

The key parameter for localized burning is burning area which is calculated based on the leading edge of the fire that depends on the fire spread rate, trailing edge which is calculated from the burnout time and width of the compartment (burning width of the fuel load). Dai et al. proposed to infer the leading edge velocity from fire tests, which suggested that the burning speed is dependent on the ventilation conditions as well [81]. Clifton [75] assumed a burning rate of around 8 mm/s for low ventilation conditions. The burnout time was calculated using the same equation (Equation 44) as used by Stern and Rein [68]. Furthermore, the location of the fire (required for the localized fire model) is determined by assuming the fire area (A_f) as a circular source with diameter (D), which provided the centre of the fire (centre of the leading and trailing edge). Hasemi's model and the correlation with heat fluxes can be found in Eurocode Annex (C), which are put forward by Franssen et al. [57].

As Hasemi's model does not account for energy conservation, therefore energy conservation is not considered for the near field. Far field temperatures are calculated using a zone model, that gives one uniform temperature in whole smoke layer, however, enormous thermal gradients in the upper zone have been observed in experimental studies [72,73]. Uniform fire load distribution with a pre-defined trajectory of fire spread is assumed.

6.3. Models of gas to solid phase heat transfer for performance-based engineering of structural fire resistance

All models hitherto discussed are idealisations of one sort or another based on the specific fire scenarios and enclosure properties. From the previous sections it is clear that practices that were adequate a few decades ago are deficient. The adoption of the more flexible PBE approach is a widely accepted solution to this lag in engineering practice. PBE approaches promote rational methodologies for quantification of hazards and their human, infrastructural and socio-economic consequences and result in improved resilience of communities, infrastructure and business. This applies both to new construction and pre-existing buildings where through deterioration of the building fabric the active and passive safety systems

may have become compromised and the nature of hazards may also have changed. However, this change in engineering practice requires computational tools (coupled with well-designed education and training programmes) that would enable realistic simulations and better quantification of hazards and the risk implied to the built environment and its users. To achieve full PBE approach for a structure under fire, it is necessary to use realistic fire models as inputs to the thermal and thermomechanical models.

To date, the most realistic representations of enclosure fires can only be obtained through simulations using computational fluid dynamics (CFD) in the context PBE, which may require multiple realistic fire scenarios to be considered. However, given the complexity and effort involved, this is not considered a practical approach for structural fire resistance design. Another considerable impediment is the tediousness of applying the highly non-uniform CFD simulation-based heat flux boundary conditions to structural components. This section describes efforts underway to automate this process.

Work on coupling realistic fire models with structural models accelerated after the World Trade Centre (WTC) disaster in 2001 to better understand the structural response to fire. Usmani et al. [82] investigated numerically the collapse of WTC Towers 1 & 2, where only the effects of fire were considered in the simulation of structural failure ignoring the damage caused by aircraft impact. Authors proposed a generalised exponential gas phase time-temperature curve (Equation 48) to calculate the time varying heat fluxes by using gas temperatures, where both convective and radiative fluxes were included,

$$T(t) = T_0 + (T_{max} - T_0)(1 - e^{bt}) \quad (48)$$

where $T(t)$ is the gas temperature at any time 't', T_0 is ambient temperature, T_{max} is the maximum temperatures achieved in the compartment and 'b' is the arbitrary 'heating rate'. To calculate the heat fluxes authors [82] performed the parametric study for a range of heating rate ('b' in Equation 48) and maximum temperatures to model structural behaviour for the various fire scenarios described by Torero et al. [83]. Using standard and parametric curves as an input in FEM models many researchers achieved PBE. Lim et al. [84] used ISO-834 standard fire gas temperatures as fire load for thermal analysis and numerically analysed concrete floor slabs exposed to fire using finite element software SAFIR [85]. Liew et al. [86] used the NFSC curves rather than conventional ISO standard fire curve, for analysing a 3D multi-story building subjected to compartment fire. Franssen [87] also investigated 3D temperature fields in steel joints using SAFIR [85] as FEM model. Jiang et al. [88] used OpenSees [89] (an open-source software) for thermomechanical analysis of structures under fire. In Jiang's study, a tool named SIFBuilder mapped the temperature histories resulting from a chosen idealised fire used a boundary condition to structural components after processing through a heat transfer analysis module. SIFBuilder includes a number of well-established fire models namely; Eurocode I [11], post flashover, hydrocarbon fire and Eurocode parametric curves, localised fire and travelling fires (section 6.2.3), where gas temperatures are used to calculate the heat flux boundary conditions. Fixed values of emissivities and convective heat transfer coefficients are used to determine the heat fluxes.

To facilitate PBE solutions for structural fire resistance, three models are required (a) fire model, which may also be obtained from a CFD simulation; (b) thermal or heat transfer model to obtain the temperature evolution history of all relevant structural components; and (c) thermomechanical model to determine the nonlinear structural response in terms of deformations and damage. The coupling of all these models is a complex problem. The key complexity in simulating the structural thermomechanical response during fire arises from the enormous difference in the relevant length and time scales associated to fire and structural models. This leads to significantly different computational approaches involving very different grid

configurations and resolutions in both spatial and temporal domains. These issues are discussed in detail in the following sections.

6.3.1. Fire structure interface (FSI)

Prasad and Baum [90] used a radiative heat transfer model to demonstrate the effects of fire on a structure (the WTC towers). The authors assumed the gas to be '*grey*' where mainly soot particles emit and absorb thermal radiation. For simplification, authors divided the compartment into two zones i.e. hot upper layers (hot zone) and relatively 'cold' lower layers (cold zone). Spatial average of temperatures and absorption coefficients were taken over vertical layers, whereas temporal averages were based on structural properties.

Radiant fluxes were calculated in the upper layers assuming uniform thermal properties. As shown in Figure 8 optical depth was integrated in the vertical direction assuming that soot is optically thick enough to neglect the effects of non-local radiations. For each vertical layer, only local radiation effects were considered (small optical depth, $\kappa L >> 1$) in the horizontal direction. This method is applicable only for conditions where temperatures are homogenous in upper layers and soot is thick enough to consider emissivity of 1.

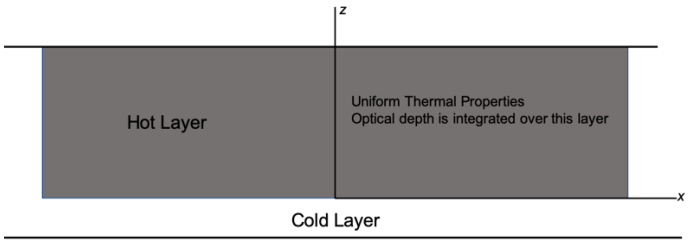

Figure 8: Upper and lower layer of Prasad and Baum [90]

Radiative transport equation is used to determine the fluxes which includes two parameters i.e. temperature and optical depth (depending on soot volume) as shown in Equation 49. If there are thermal gradients along the length, then the proposed method would not provide the true fluxes. Similarly, if the soot layer is thin (large optical length) the emissivity (ϵ) would not reach 1, and local radiation can't be considered which is quite common for large spaces as discussed in section (6.2)

$$\frac{dI}{dz} = \epsilon\sigma T^4 - \kappa I \tag{49}$$

where in Equation 49, I is the radiative intensity, and κ is absorption coefficient.

In addition to the above assumptions, to calculate the convective fluxes on the surfaces, a fixed value of heat transfer coefficient (h_c) was considered (25W/m^{2}k) [91], however, h_c varies with characteristic length scales of the structural component cross-sections and local velocities [92]. The value of h_c is quite large for very small characteristic lengths, therefore it may potentially be very high for flanged sections and truss elements [93]. Prasad and Baum mentioned that to determine the convective fluxes local instantaneous temperatures at upper layers were taken as bulk temperature, however, the optical depth is not mentioned (integral of z) whereas CFD grid size was 50cm. If the optical depth is larger than this (which it is likely to be), the value of bulk temperature would be much lower than the average temperature of soot layer as shown

in Figure 9 (deduced by the Prasad and Baum). Moreover, if the soot layer is not thick enough in the far field, the radiation losses would be higher and other products of combustion would come into play e.g. water and CO_2, and it is a known fact that emissivity of CO_2 and water varies with temperature [94].

Based on the assumptions and applicability of the model to calculate the radiant fluxes, this model belongs to the same category as of classical and parametric curves where one uniform temperature (averaged or maximum) with unit emissivity can be assumed and a fixed value of convective heat transfer coefficient can be considered.

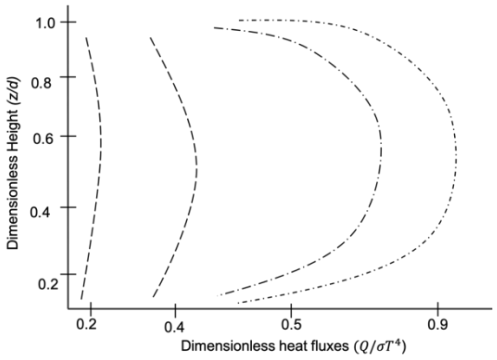

Figure 9: Heat flux profiles with height, where *d* is depth of upper layer [90]

6.3.2. Adiabatic surface temperature

The concept of Adiabatic Surface Temperature (AST) was first introduced by Wickström [95]. AST represents the surface temperature of a perfectly insulated surface when exposed to the same conditions as the real surface. In terms of fluid-structure interface, AST can be considered as fluid phase temperature that can be employed to calculate both radiation and convection heat transfer by employing certain number of assumptions (discussed later in this section). The author demonstrated how a single quantity (AST) can be transferred from the fluid domain to the FEM model as an effective boundary condition. Since the introduction of AST, it has been frequently used by researchers to study structural behaviour (sometimes without explaining its applicability and assumptions [96–98]). Before going further, it is important to begin with understanding the heat transfer phenomenon between the solid domain (structure) and fluid domain (gas phase),

During fire, the total heat flux ($\dot{Q}_{total}$) over a surface is the summation of incident radiative flux ($\dot{Q}_{radiative}$) and convective heat flux ($\dot{Q}_{convective}$) as shown in Equation 50.

$$\dot{Q}_{total} = \dot{Q}_{radiative} + \dot{Q}_{convective} \tag{50}$$

Effective radiative fluxes on the surface can be written as the difference of flux incident on the surface and fluxes emitted from the surface (Equation 51).

$$\dot{Q}_{radiative} = \varepsilon \left(\dot{Q}_{incident} - \sigma T_{surface}^{4} \right) \tag{51}$$

Incident fluxes can be written as the summation of all fluxes (Equation 52) incident on the surface from all direction. In equation 52, ε represents the emissivities of all sources flame and F denotes the configuration factors (view factor or geometrical factor).

$$\dot{Q}_{incident} = \sum_{i} \varepsilon_i F_i \sigma T_i^4 \tag{52}$$

Wickstrom simplifies the model by assuming the emissivity of soot as unity and configuration factors as one, so that incident flux can be written as in Equation (53). Unit emissivity implies that the surface is fully engulfed with smoke, and a unit configuration factor represents that the surface receives radiation from all directions. The implications of these assumptions are very significant and were discussed in detail by Torero [99]. Thus, it is important to understand that this approach cannot be seen as universally applicable. It is particularly important to note that these assumptions would be invalid where soot density is low, and structural surface is concave (configuration factor would be lower than one).

$$\dot{Q}_{incident} = \sigma T_{radiative}^4 \tag{53}$$

Where, $T_{radiative}$ is radiation temperature.

Radiative fluxes can be written as equation 54, where h_r is the radiative heat transfer coefficient:

$$\dot{Q}_{radiative} = h_r\left(T_{radiative} - T_{surface}\right) \tag{54}$$

Convective heat fluxes over the surface depend on the difference of gas temperature and surface temperature:

$$\dot{Q}_{convective} = h_c\left(T_{gas} - T_{surface}\right) \tag{55}$$

Equation 50 can be rewritten as:

$$\dot{Q}_{total} = h_r\left(T_{radiative} - T_{surface}\right) + h_c\left(T_{gas} - T_{surface}\right) \tag{56}$$

By assuming the surface as adiabatic boundary (perfectly insulated) with the same emissivity and heat transfer coefficient as of the real surface, the total fluxes on the adiabatic surface would be zero as represented in Equation 57, where T_{AST} is the temperature of adiabatic surface.

$$h_r(T_{radiative} - T_{AST}) + h_c\left(T_{gas} - T_{AST}\right) = 0 \tag{57}$$

Now, the total heat transfer at the surface (Equation 56) can be calculated by subtracting Equation 57 in terms of effective boundary temperature (AST).

$$\dot{Q}_{total} = h_r\left(T_{AST} - T_{surface}\right) + h_c\left(T_{AST} - T_{surface}\right) \tag{58}$$

According to Equation 58, only ASTs are needed to calculate the heat fluxes over the structure for heat transfer analysis. The time variant AST can be obtained from the fire modelling (CFD) and then can be transferred for structural calculations.

Above equations from 50-58 explain how the net heat flux can be inferred from the AST, however, it is necessary to understand how the AST is calculated from CFD. The expression in Equation 52 for the incident radiation shows that the incident radiation flux depends on the configuration factor (geometrical factor, F) and emissivity of gas. As discussed earlier, Wickström assumed the configuration factor as 1, which means that a surface receives the entire radiant fluxes from all sources. Moreover, total emissivity of gas considered as 1 as well, in reality the emissivity depends on optical length (Equation 59). The authors assumed that soot is thick enough (small optical depth) that allows them to assume unit emissivity. This is equivalent to reducing all emitting sources to one i.e. smoke which is fully enveloping the structural member. The analysis by Torero [99] shows that this approach is equivalent to assuming an emissivity of zero for the furnace gas and a Biot number much greater than unity for the furnace linings when conducting a standard furnace test. The authors link the present T_{AST} approach to the use of a plate thermometer in the furnace tests. While there is a relationship, this relationship is defined by the assumptions within the analysis.

$$\varepsilon = 1 - e^{-\kappa L} \tag{59}$$

where ε is emissivity, and κ and L are the extinction coefficient and path length, respectively.

Although the AST concept is a robust, practical and simple method to obtain surface boundary conditions for thermal analysis, it is applicable only for the conditions where optical depth is thick enough to assume a single radiative source, emissivity of unity and therefore radiation losses from the surface can be neglected and local conditions for heat fluxes can be considered.

The analytical solution to determine the AST in FDS: a widely used CFD package for fire simulation, can be found in [100] and FDS User's guide [101]. FDS can compute and provide an output file containing ASTs by integrating both gas temperature and radiative heat fluxes from all directions. So, basically, AST contains the information on radiative heat transfer from all surfaces and convective heat transfer of adjacent gases. It is important to note that the computation of the AST by FDS does not require the assumptions of the analysis for the emitting sources, so in reality it is only using these assumptions to neglect surface radiative losses. Although this method provides a simple way to obtain thermal boundary conditions for the heat transfer analysis in an FEM model, a user must be able to understand where T_{gas} (gas temperature) and $T_{radiative}$ (radiation temperature) can provide a better averaged value. For example, while evaluating temperatures at the lower part of the room such as base of columns, due to optical thin environment radiation would be less effective and the value of emissivity of gas would be lower than one, so $T_{radiative}$ might be poorly averaged in the CFD grid. Similarly, at the upper part of fire compartment, gas temperatures might not be averaged correctly. While calculating from FDS, heat transfer coefficient needs to be provided, Sandström [102] in his thesis proposed a numerical scheme (based on heat balance) to calculate the radiation and convective heat transfer separately within FDS itself, where variation of convective heat transfer coefficient with velocity and length was considered, however the method was not validated.

In CFD calculation, by placing the AST thermocouples along the length of the structural member thermal gradient can be predicted. The AST concept can be used with any fire scenarios, such as, localized fire [103,104] and real fire incidents [105], refer to Table 4. The results, however, for localized fire or travelling

fire may be conservative because practically it's not possible to have unit gas emissivity in the far field (away from the flaming zone) and in optically thin environment other products of combustion may come into play.

6.3.3. Jowsey's framework for extracting boundary heat fluxes from CFD

Jowsey [93] investigated convective and radiative heat fluxes derived from CFD simulations (using FDS) at the solid boundaries and over the surfaces of structural components in his PhD thesis. To quantify the heat fluxes on the structural surfaces his assumptions were:

- Structural members are fully engulfed by the smoke layer.
- Post-flashover conditions prevail so the fire can be considered fully developed.
- Compartment emissivity is dominated by soot particles rather than CO_2 and water.
- Structural surface is considered cold, therefore no radiative feedback from the surface was considered.

Jowsey's framework is basically a post-processing tool that can use the outputs (gas temperatures, velocities, extinction coefficients) from FDS (or from any other suitable CFD tool) and determines the heat flux at the solid gas-solid interface boundary (by implication on surfaces of structural components) to use as boundary condition for heat transfer into the solid. Jowsey's model is able to capture the variation in the values of convective heat transfer coefficient due to length scale and local gas phase velocities. It was found from his work that the variation of convective heat transfer coefficient with temperature, length scale and local velocity was similar irrespective of shape or geometry. To determine radiative fluxes from the gases on the surfaces, Jowsey uses the gas temperature and local emissivity. He calculated optical depth (Le = 1/k) based on local extinction coefficient to evaluate optical thickness. A hemispherical control volume (as shown in Figure 10) where local gas radiation can be considered is defined. A series of hemispheres (shells) are examined for the presence of smoke. The radius of a hemisphere can be determined from the path length by evaluating the extinction coefficient at each shell radius. The radius of the final shell where the radiant intensity at the surface reaches to an acceptable error limit would be the hemispherical radius of the control volume. Within the final shell volume constant properties of gas can be considered that can be averaged at a point source on the surface. Thus, this model is able to capture the thermal gradients along the length of structural member.

Before performing his analysis, Jowsey defined the characteristic heating time for the structural materials based on the Biot number that defines if the structure is thermally thick or thin, and other properties such as specific heat and density. It enables establishing time-intervals over which heat fluxes can be averaged, which consequently reduces the computational time of conduction heat transfer without losing the level of accuracy.

The Jowsey's model is capable of providing better results for fire scenarios where the fire environment is optically thick, which is again more applicable to ventilation controlled fires. For optically thin fires where soot concentration is lower than CO_2 and water, the grey gas assumption would over-predict the emitted radiation. However, in order to calculate the convective heat transfer coefficient, Jowsey's model is quite robust in comparison to others.

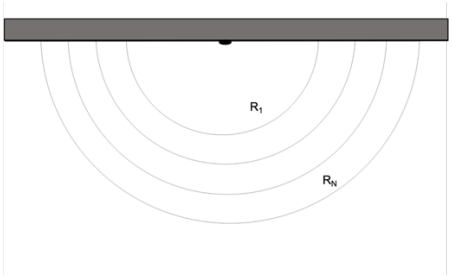

Figure 10: Control Volume of Jowsey's model to calculate the optical depth

Table 3: A summary of fire models used in CFD-FEM couplings

Models	Simplification/Assumption	Features	Limitation
FSI	-Spatial average of quantities in vertical direction -Uniform thermal properties in upper layers -very thick soot in upper layers	-provide realistic results from a CFD model - can define the thermal gradients in vertical direction	-does not provide thermal gradients in horizontal direction, so basically employed homogenous condition over the surface -would provide over-conservative results for travelling fire
AST	-consider view factor value as one - emissivity of soot particles as one	- it includes the information of convective heat transfer and radiative fluxes from all surfaces - easy to apply as only one quantity to transfer to model -FDS itself can calculate and provide an output file containing temporally ASTs values	-conservative results where surface is concave or optical depth is large -may provide conservative results for localized or travelling fire
Jowsey's framework	-fully engulfed condition - fully developed fire -No radiative feedback from the structural surface	-a post processing tool which just takes outputs from any CFD tool -provide more realistic heat fluxes based on local conditions -calculation for convective heat from the velocities obtained from CFD	- conservative results for optically thin environment

6.4. Current research on CFD-FEM coupling

Over the last two decades, considerable research has been done to couple CFD with FEM. In addition to various kinds of fire scenarios (localised fire, pool fire), different types of structures such as tall buildings, tunnels, and bridges were also investigated. Table 4 provides a selection of some of this work in chronological order. Hamins et al. [106] and Pantousa et al. [107] used Prasad and Baum's FSI model to determine the surface temperatures. Others used the AST method for compartment fire, localised fire as well as for pool fire [96,103,104,108–112]. Welch et al. [113] paired a number of CFD and FEM software to analyse structures in fire. In Welch's models, the data from the CFD calculations were interpolated based on the geometry created by FEM to identify the configuration factors. Radiative fluxes, gas temperature and heat transfer coefficients were directly calculated from the CFD calculation.

Table 4 provides information on types of coupling, validation studies and software used for fire modelling and structural analysis.

Table 4: A summary of some surveyed research for coupling of CFD with FEM

Author	CFD-FEM Software	Coupling Type	Coupling method	Test/Validation
Prasad and Baum [90] **2005**	FDS -ANSYS	One-way	FSI (section 6.3.1)	The collapse of the WTC towers had been studied for the failure of trusses under heptane pool fire
Hamins et al. [106] 2005	FDS -ANSYS	One-way	FSI	An experiment had been conducted in a compartment where steel elements (trusses) are present
Jowsey [93],2006	FDS- (calculate only heat fluxes using MATLAB	One-way	Develop a framework (section 6.3.3)	Cardington Test [70] was validated and compared with Eurocodes
Wickström et al. [95] 2007	FDS -ANSYS	One-way	AST (section6.3.2)	NIST test for the WTC investigation
Duthinh et al. [114], 2007	FDS-No Information	One-way	AST	NIST test for the WTC investigation
Welch et al. [113] (2008)	VESTA, SOFIE, JASMINE and FDS for fire and DIANA, ANSYS, SAFIR and STELA for FEM	One-way and two-way	A few numbers of framework were suggested based on couplings (No correlation)	localised fires in a large compartment and a large open car-park structure exposed to transient fire
Banerjee et al. [108] 2009	FDS -Abaqus	One-way	AST	Beam in the room under localised fire
Baum [115],2010	FDS -ANSYS	One-way	FSI	The collapse of the WTC had been studied with impact analysis on WTC
Tondini et al. [116–118] 2012, 2015	FDS - SAFIR	One-way	Direct data from FDS i.e. gas temperatures and radiant heat fluxes using interpolation (No correlation)	Conduct an experiment on beam under pool fire for mechanical response and assess the effect of flame emissivity
Alos-Moya et al. [105] (2014)	FDS -Abaqus	One-way	AST	Validate with case study and data obtained from ALDOT for bridge failure. And compare with standard curve
Pesavento et al [119,120], 2014, 2018	FDS - Comec-HTC	One-way	AST	A numerical study for a fire in Brenner Base Tunnel (between Italy and Austria) was conducted
Silva et al. [121] (2016)	FDS -ANSYS	one-way	AST	H-profile column is exposed to a localised fire
Zhang et al. [111] (2016)	FDS -ANSYS	one-way	AST	simulation and validation of the experimental data (Kamikawa et al. [55])
Li et al. [103] 2016	FDS -ANSYS	one-way	AST	compares with experimental data of Hasemi's localised fire model
Malendowski et al. [122] 2017	FDS -Abaqus	one-way	AST	Geometry of by Pyl et al. [123] was utilised for testing the model
Hofmeye et al. [104] 2018	FDS -Abaqus	Two-way	AST	A steel facade in a compartment under localised fire

6.4.1. Coupling methods

A comprehensive study for coupling methods can be found in an article of Welch et al. [113]. One-way coupling is considered adequate, Navier-Strokes equations are solved first for the fluid or gas phase usually assuming adiabatic boundaries. Outputs (temperatures, emissivity, heat transfer coefficient etc.) from the CFD simulation are then used as input as boundary conditions for the solid domain and heat transfer analysis is conducted to obtain the thermal response history in the solid domain (which includes structural components like beams, columns, trusses). Finally, the temperature history of the structural components obtained from the thermal analysis is used to carry out a thermomechanical response analysis provided deformations of the structural system. Where two-way coupling is considered necessary, the problem becomes more complex and requires an iterative solution. This approach is naturally more accurate and enables the heat losses into the solid domain during the fire growth phase (and heat gain from the solid domain during the decay phase) to be accounted for. This accuracy, however, comes at a significantly increased computational cost and user effort. Table 4 highlights some of the coupling approaches used recently.

Although there have been many attempts to couple CFD and FEM simulation (Table 4), the complexity associated with the coupling the fire models with the structural response models has not yet yielded a satisfactory solution. Torero et al. [124] explained the importance of Biot number in defining the thermal boundary conditions for structures in fire.

7. Classification of Models

As a result of this study, all fire models can be categorized based on their applicability for particular fire scenarios. We classified them in three major categories as represented in Table 5. The first category includes the fire models that represent the idealized uniform fire scenarios, which is further divided into three sub-categories (IA, IB, and IC). Category IA represents the group of fire models or fire curves which are used for the fire scenarios where structural components are fully engulfed in fire, and only one spatial temperature (at a specific instant of time) is required for studying the thermomechanical response of the structure. However, these curves do not include the physics embedded within the fire dynamics and heat transfer in the fire compartment. Thus, the curves are universal, independent of scenario. The fire models in Class IB provide only one steady state maximum temperature that can be used as a thermal boundary condition for structural analysis for a specified period of time. These curves include a simplified description of both fire dynamics and heat transfer. The last sub-category (IC) includes the fire curves with time-variant temperatures. By realising the time dependency, these curves do not add additional physics to category IB but simply provide a more refined, data-based representation, of category IB. The correlation and idealisations that are used to represent the non-uniform temperature distributions such as localised and/or fuel-controlled fire scenarios are grouped in Category II; finally, Category III includes the methods that can be used to characterize the temperatures (thermal boundary) for the structures in real fires.

Standard Time-Temperature curves such as ISO, ASTM that are widely used to determine the structural fire resistance for compartment fires are included in Category IA. The fire models in Category IB represents the ventilation-controlled fire scenarios. As discussed above, category IB contains the curves that provide a single value of the temperature for the fully developed fire scenarios such as the fire models proposed by Kawagoe, Thomas, and Law. The fire models in Category IB do not provide any information for the decay

phase of the fire. On the other hand, the fire models in Category IC specified the uniformly distributed time-variant temperatures for the whole fire process including growth and decay phase of the fire. Parametric fire curves in Eurocode 1, zone models, and the methods of Magnusson and Thelandersson fall in this category.

To determine the realistic thermal boundaries on a structural surface either a field model (CFD) or time-evolving temperatures from experiments can be used. The methods that are used to determine the thermal boundary condition from the CFD are grouped in Category III such as AST, FSI, and Jowsey's model.

Structural fires can be defined as compartment fires, localised fires, travelling fires or real fires as shown in Figure 11 (Figure 11 summarises Table 5). Based on the type of fire, a particular fire models can be chosen to determine the thermal boundary conditions. The idealised fire models that provide uniform temperatures (IA, IB, and IC) are generally used to evaluate the thermal boundary conditions in compartment fires. To define travelling fires, the available idealisations use the fire models from category I and II. It is worth noting that the models ETFM uses zone models (Category IB) and localised fire models to determine structural temperatures, however zone model alone cannot represent fires in large open spaces where fire may be fuel controlled. Therefore, the fire models for travelling fires are classified in category II.

While defining real fires, a CFD model is able to represent the physical model and provide a realistic time-temperature history. Using any of the methods of calculating gas and solid phase heat transfer such as FSI, AST thermal boundary conditions can be obtained for such fires.

Table 5: Classification of fire models

Category			Description	Models
Idealized Models	Uniform	IA	Uniform temperature, all structural components are engulfed in fire, fully developed and no cooling phase described	ISO, ASTM, Hydrocarbon curves
		IB	One steady state maximum temperature over a period of time, ventilation controlled, fully developed fire, uniform temperature	Kawagoe, Thomas, Law, Babrauskas,
		IC	Time-variant temperatures, uniformly distributed temperatures, represents the cooling phase of fire development as well.	Magnusson and Thelandersson, Pettersson, Parametric Curves in Eurocode I, zone models
	Non-uniform	II	Localised fires, fuel controlled, travelling fires	Hasemi's Model, Rein's model, ETFM
Realistic		III	Realistic temperature distributions	Experiments, field models (FSI, AST methods)

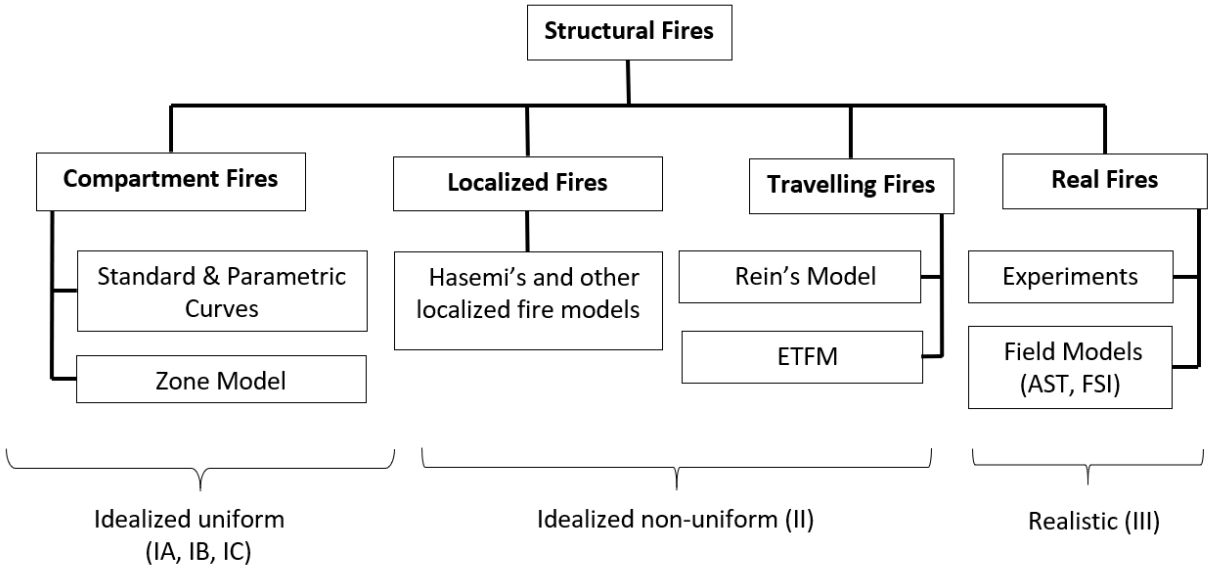

Figure 11: Classifications of the fire models used for structural fire resistance

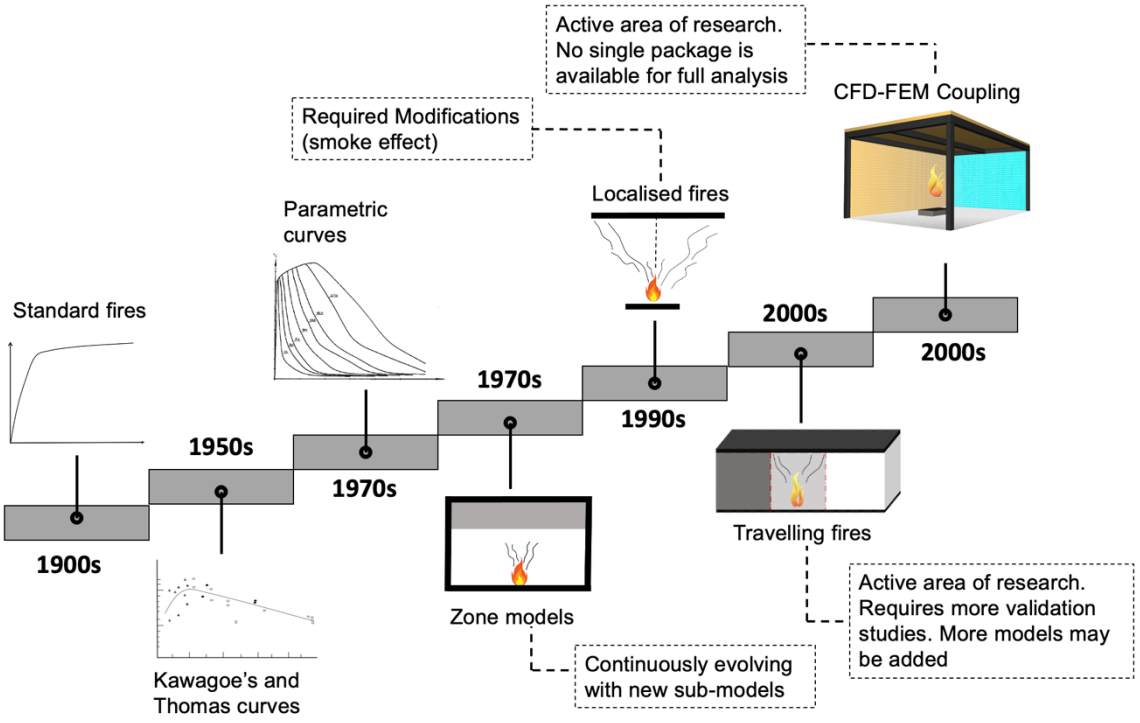

Figure 12: History of fire models and current development

8. **Current Development and Challenges**

It is clear from the previous discussion that over the last century the field of structural fire safety has seen a great deal of progress (Figure 12). However, it is still evolving and demands better models to represent realistic fire scenarios in the context of PBE. Some knowledge gaps and challenges associated with PBE for structural fire engineering are discussed in this section.

8.1. **Computational models for PBE**

In designing structures to resist fire, prescriptive fire loading (standard curves) does not account for any factors affecting the fire behaviour or how these factors might affect structural performance. Estimating realistic fire scenarios is an important prerequisite for the development of the PBE approach. In the past CFD has been considered as the most suitable approach for estimating realistic gas phase boundary conditions in order to determine solid phase thermal history. As discussed in section 6.4, the CFD-FEM coupling problem is one of the most extensively researched in past two decades. This type of integrated computational framework addresses the need for significantly better simulation tools for structural and fire safety engineers to encourage wider acceptance of PBE concepts. Currently, there is no single package capable of modelling the full sequence of a fire scenario, heat transfer to the structure and the thermomechanical response of the structure. There are commercial and open source software tools capable of modelling the relevant phenomena individually, nevertheless, they all have constraints and include assumptions that do not necessarily allow for seamless coupling of the models. Some of the most popular structural fire engineering software (e.g. SAFIR, Vulcan) are typically not open source therefore, the basic modelling approach cannot be changed. Authors have focused on developing open source software for structural fire engineering using the OpenSEES software framework [92]. An open-source model for CFD-FEM coupling problem has also recently developed by the authors, namely; OpenFIRE (can be downloaded from [125]) which enables users to get data from a CFD tool and apply to an open source structural analysis software (OpenSEES).

It is worth noting although CFD-based fire modelling has been used extensively, it has been reported that CFD simulations are highly sensitive to certain parameters which are essential to the necessary outputs [69]. Therefore, the user must have good knowledge and understanding of the uncertainties involved in the CFD modelling and must have adequate information about the fire spread phenomena and fire dynamics involved within the building to determine realistic fire scenarios. While generating a computational model that represents the physical world, the designer must have understanding of the physics and chemistry embedded with the CFD models otherwise, as Merci and Beji [126] stated, that without understanding the fluid dynamics or familiarity with physical and numerical modelling these computational packages would just be a ‘black box’ with “colourful images”.

8.2. Travelling fire models

Over the last decade, a number of travelling fire tests have also been carried out to investigate the travelling behaviour of fires in large compartments, including the Veselí Travelling Fire Test in Czech Republic in 2011[127] , tests at BRE laboratory in 2013 [128], Tisová Travelling Fire Test in the Czech Republic in 2015 [129], Malveira fire test in Portugal in 2017 [130]. The objective of the tests was mainly to understand the fire behaviour but some of them had a special focus on the thermal input for structural response. These tests are being used to validate some of the analytical models [80].

Until now all travelling fire tests have used either wood or hydrocarbons as fuel, so the chemistry embedded with these tests is limited to these fuels although it is clear that chemical composition of fuel would affect the amount of heat generation as well as spread rate. Travelling fire tests are essential for introducing idealised fire models for large indoor spaces where compartment fire assumptions are not valid. Travelling fire models are potentially a more realistic alternative to using CFD for in a PBE context as multiple scenarios can be rapidly generated. It is many times more important to consider multiple fire scenarios in PBE that envelop the fire load on the structure more effectively than an expensively obtained single CFD scenario. However, more travelling fire models are required in future as there is further development work needed for such models.

8.3. **Localised fire models**

The current localised fire models only include heat flux from flames (refer section 5.5), the effect of smoke layer is not considered. In an experimental study performed by Wakamatsu et al. [131], it was found that due of the presence of soffits the entrapped smoke raised the temperature of structural component (beam) significantly. In the Malveira travelling fire test [130], it was observed that as soon as fire reached near the beam soffit temperature raised drastically and the radiation feedback from the smoke changed the fire behaviour from travelling to fully developed fire. Beam soffits are common in modern buildings especially in large compartments where fire may accumulate and generate a deep smoke layer. More tests are needed to determine modifications to the current localised fire models by quantifying additional heat flux generated by the thick smoke layer.

In another module of OpenFIRE: 'OpenFIRE for idealised fire' allows the user to apply idealised fire models for structural analysis. Being open source, it gives freedom to the user to make changes or add new models. It can be downloaded from [125].

8.4. **Bridging the two disciplines**

Fire engineering and structural engineering are two distinct domains and the interaction between them has hitherto been quite small [132]. As Buchanan stated, "Fire engineers and structural engineers need to talk to each other much more than they do now". Some of the key gaps are mentioned in this section which requires both disciplines to work together and advance the field of 'structural fire engineering towards promoting PBE.

- The nature of the combustibles defines the kinetics of chemical reactions which in turn dictates the growth rate of the fire [60,94]. Therefore, it is vital to identify the material composition of the fuels stored in a compartment. Multi-material testing should be considered for large fires. Some tests for office type of occupancies were conducted by NIST to reconstruct the fires associated with the collapse of the WTC towers [133].
- Various studies have emphasised on the effects of fire load and ventilation on fire behaviour [5,31,134], however, not enough attention has been paid to the effects of fuel distribution and its packing and building geometry. Arrangement of the fuel also plays an important role in determining the fire spread rate and severity of the fire. In the case of the collapse of the Plasco Building, it was found that due to the height of the fuel fire spread vertically and reached the top floor in the 15 storey building (the fire was initiated at the 10th floor) within 25 minutes [135]. This rapid growth in fire lead to the collapse of the building within 3.5 hours.

- In fire investigation and forensic analysis for reconstructing a fire, conventional methodologies described in codes and textbooks are limited to "cause and origin" [136,137]. These methodologies include scientific procedures that provide guidance for thermochemical decomposition of combustibles [60,94], and ignition procedure theories [138] but do not methods to determine the thermomechanical deformations of solids and structures that could be used to determine the reasons for structural collapse. Improved understanding of thermomechanical and structural response can lead to improved designs of structural fire safety and fire resistance systems. The most extensive and detailed forensic study was performed by NIST for the collapse of three towers of WTC (1,2 and 7) [62,139], however these methodologies were ad-hoc and were improvised during the investigation [140]. Reconstruction of a fire for a forensic analysis should be based on the realistic fire in order to develop a rational hypothesis.
- In recent years there is rapid growth in the use of timber as structural material for tall buildings [141]. Timber is itself a combustible material and will add to the fire load. The burning characteristics of timber are quite complex and include charring and smouldering which are difficult to model [132]. Modelling of themo-mechanical behaviour of timber is also currently evolving. Traditional design frameworks that use a predefined temperature vs time curve as the source of the thermal load assume that once the building contents have been consumed (i.e. burn-out) the structure does not continue to burn. This forces the understanding of self-extinction as a necessary outcome for timber structures [22]. Instances like the recent fire accident at a motorcycle museum in Austria (January 2021), where the whole structure which was constructed using timber burnt to the ground [142], raise doubts about the current design methods for timber structures. Understanding the safety of timber structures can therefore also require understanding what are adequate levels of inherent passive fire resistance which requires a great deal of fundamental research to enable reliable quantification necessary for PBE.

9. **Performance level**

According to Hertz, "safe design" of a structure in terms of fire depends on two important questions: first, if the building is allowed to collapse during fire (which is generally never an acceptable criterion set by a code) or not, second; if the stakeholders rely on the fire brigade [51]. It is through stakeholder agreement that the performance requirements are set. Performance requirements not only involve defining what is unacceptable level of behaviour for the structure, but in the case of fire, they also require to define expected intervention of stakeholders such as the fire brigade or building management. While many times there is confusion with regards to what are the quantitative metrics that define acceptable performance, what is clear is that testing a design for performance requires modelling the fire. Furthermore, in the case of structural behaviour it requires modelling the thermal impact of the fire on the structure.

It is common that the approach is for structures to be designed to resist fire for a specified 'design fire.' Performance level of a design can be considered "achieved" if the structure is able to resist the 'design fire.' The meaning of 'resist' is quite simple if standardized test metrics are used but can be extremely complex if PBD metrics are required.

As an example conceptual performance requirement matrix based on the 'hazard level' and 'probability of occurrence of fire' is presented in Table 6. A building can be designed to resist to four damage levels that can be set as acceptable performance level; superficial damage, minor damage, major damage, and total collapse. Probability of fire occurrence can be quantified based on frequency of structurally significant fires (f_s) (NFPA 557 [24], calculated based on statistical surveys). Hazard levels can be categorised as high hazard, medium hazard, and low hazard based on the fuel load for a particular occupancy such as high fuel load, medium fuel load and low fuel load, respectively. It is similar to the hazards defined in NFPA 13

[143] for active fire protection of a building (light hazard, ordinary hazard, and extra hazard). The amount of heat generation depends on the fuel load. Evidently, design requirement would be lower for a low hazard area. Based on probability of a fire and hazard level performance criteria can be estimated; for instance, if a building falls under high hazard and the probability of fire in those buildings is low in such case buildings can be designed only for superficial damage. Similarly, if a building falls in the category of low hazard and probability of fire is very high, due to the lower fuel load, the building can be designed only for minor damage. In Table 6, any design above the 'design lines' would be considered 'overdesign'. In terms of life safety, the minimum design requirement should relate to the evacuation time for occupants and cover for the inherent uncertainties of human behaviour. Therefore, it can be included with 'superficial damage' performance level (Table 6).

In prescriptive codes, design requirements for any structure are primarily based on the information obtained from idealised fire models, which provide passive protection for design fires and are expected to resist collapse during fire. However, if the structure is expected to be exposed to a minor fire (low hazard category), the fire may affect it superficially, in such a case design would be considered 'massively overdesigned'. On the other hand, if the fuel load is applied using realistic models an expected performance could be assessed and demonstrated to be achieved in all cases. However, this requires a thorough risk assessment of a structure to develop reasonable fire scenarios and to obtain the associated realistic thermal data for structural assessment. Finally, based on the required level of performance ("demand"), a designer can create fire scenarios for a particular structure to get expected performance ("supply") and avoid overdesign.

The presence of active fire protection systems such as sprinklers may influence the hazard level. Generally, the presence of sprinkler system may control the fire, but there is always a significant probability that these systems might not work. A good example could be a fire that follows an earthquake that has damaged the fire protection systems. According to a survey carried out by NFPA[144] in 2017, in 8% of fires sprinklers did not operate. Therefore, it is difficult to justify reducing the design fuel load [132] on the basis of sprinkler protection, despite this approach being implemented in Eurocode 1.

Table 6: Performance requirement for a building design based on hazard level

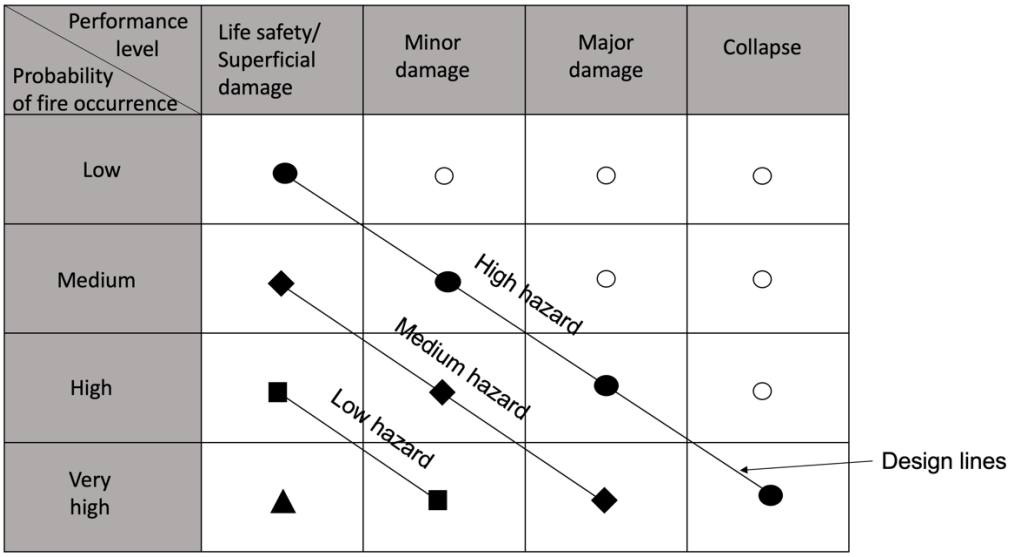

Conclusion

Over the last seven decades, a number of models have been published which have progressively enabled design of structures to better withstand fire induced loads. In the current paper, the evolution of the fire models to quantify the structural fire resistance are reviewed. The methods to determine the gas temperatures inside a compartment have evolved from idealised standard temperature-time curves to more sophisticated computational models. Most of the models for compartment fires are proposed for ventilation controlled fires, where the heat balance equation is applied to obtain structural boundary conditions. Fire models are generally simplified based on valid assumptions for particular fire scenarios, this paper discussed their suitability while using for structural fire resistance assessment. The limitations and assumptions associated with the most commonly used fire models are discussed in detail. A survey of recent advances in obtaining realistic boundary conditions for structural analysis using CFD and its coupling with FEM models is reported. Methodologies employed to couple a CFD model with an FEM model to investigate the structural response to fire are discussed which show that the proposed methods also have limitations such thermal gradients in the horizontal direction are not predicted in the FSI method or the temperatures obtained from AST method may be conservative for localised fire scenarios. However, it was found that most researchers are using the AST method for different fire scenarios from compartment fires to localised fires (bridge fires, tunnel fires) without providing any rationale for its use. To achieve full PBE solution, an open-source package is required that can perform all three analysis. The development of such a tool will also facilitate continued evolution of PBE methodologies that are fit to address the challenges and uncertainties arising from future technology driven changes including the uncertainties associated with climate change.

All models that are discussed, are classified into three categories where Category I and II represent the idealised uniform and non-uniform fires, respectively. The models used for travelling fire scenarios are also briefly discussed in the paper and categorised in category II, these models are not widely accepted in structural engineering so far, and due to lack of validation studies are not mature yet. In the near future, more sophisticated models might be required because of new architectural practises for designing innovative and large floor compartments. A conceptual framework based on the probability of occurrence of fire is proposed to evaluate the performance criteria to obtain a performance-based designs.

Acknowledgement

This research is funded by the RGC Hong Kong GRF Scheme (No. 15220618).

References

[1] A.H. Buchanan, A.K. Abu, Structural Design for Fire Safety, Second Edi, John Wiley & Sons, 2017.

[2] L. Bisby, J. Gales, C. Maluk, A contemporary review of large-scale non-standard structural fire testing, Fire Sci. Rev. 2 (2013) 1. https://doi.org/10.1186/2193-0414-2-1.

[3] S.H. Ingberg, Fire loads, Q. J. Natl. Fire Prot. Assoc. 22 (1928) 43–61.

[4] K. Kawagoe, Fire Behaviour in Rooms - Report No. 27, (1958).

[5] M. Thomas, P.H., Heselden, A. J. and Law, Fully-developed compartment fires-two kinds of behaviour, no. (n.d.) 1967.

[6] SFPE, SFPE Handbook of Fire Protection Engineering, 2016. https://doi.org/10.1016/s0379-7112(97)00022-2.

[7] SFPE, Engineering Guide - Fire Exposures to Structural Elements, Society of Fire Protection Engineers, 2004.

[8] SFPE, Engineering Standard - Calculating Fire Exposures to Structures, Society of Fire Protection Engineers, 2011.

[9] J.L. Torero, A. Law, C. Maluk, Defining the thermal boundary condition for protective structures in fire, Eng. Struct. 149 (2017) 104–112. https://doi.org/10.1016/j.engstruct.2016.11.015.

[10] NFPA 557 : Standard for the determination of fire loads for use in structural fire protection design, 2020.

[11] EN 1991-1-2, Eurocode 1: Actions on structures - Part 1-2: General actions - Actions on structures exposed to fire, Eur. Commitee Stand. (2005).

[12] S.H. Ingberg, J.W. Dunham, J.P. Thompson, Combustible contents in buildings, 1957.

[13] C.G. Culver, Survey Results for Fire Loads and Live Loads in Office Buildings., Natl. Bur. Stand. (1976).

[14] T. Araújo, S. Vieira, T. Ribeiro, Analysis of structural integrity of a non-completed 28 year-old building in the city of Patos de Minas (MG), J. Build. Pathol. Rehabil. 1 (2016) 1–12. https://doi.org/10.1007/s41024-016-0018-1.

[15] B.S. Kumar, C.V.S.K. Rao, FIRE LOADS IN OFFICE BUILDINGS, J. Struct. Eng. 123 (1997) 365–368.

[16] National Fire Protection Association (NFPA). Validation of methodologies to determine fire load for use in structural fire protection – final report. The fireprotection research foundation – research in support of the NFPA mission., 2011.

[17] C.G. Culver, J. Kushner, A program for survey of fire loads and live loads in office buildings, Natl. Bur. Stand. (1975).

[18] T. Caro, J. Milke, A survey of fuel loads in contemporary office building., NISTGCR- 96-697. (1996).

[19] P.H. Thomas, Design guide: Structure fire safety CIB W14 Workshop report, Fire Saf. J. 10 (1986) 77–137. https://doi.org/10.1016/0379-7112(86)90041-X.

[20] O. Pettersson, S. Magnusson, J. Thor, Fire Engineering Design of Steel Structures. Bulletin 52, 1976.

[21] R. Emberley, A. Inghelbrecht, Z. Yu, J.L. Torero, Self-extinction of timber, Proc. Combust. Inst. 36 (2017) 3055–3062. https://doi.org/10.1016/j.proci.2016.07.077.

[22] A.I. Bartlett, R.M. Hadden, J.P. Hidalgo, S. Santamaria, F. Wiesner, L.A. Bisby, S. Deeny, B. Lane, Auto-extinction of engineered timber: Application to compartment fires with exposed timber surfaces, Fire Saf. J. 91 (2017) 407–413. https://doi.org/10.1016/j.firesaf.2017.03.050.

[23] R.J. HART, J. 0. LEE, D.J. BOYLES, N.R. BATEY, The Summerland Disaster, Br. Med. J. (1975) 256–259.

[24] NFPA557, NFPA 557 : Standard for the determination of fire loads for use in structural fire protection design, (2020).

[25] N.E. Khorasani, M. Garlock, P. Gardoni, Fire load: Survey data, recent standards, and probabilistic models for office buildings, Eng. Struct. 58 (2014) 152–165. https://doi.org/10.1016/j.engstruct.2013.07.042.

[26] N. Elhami-Khorasani, J.G. Salado Castillo, T. Gernay, A Digitized Fuel Load Surveying Methodology Using Machine Vision, Fire Technol. (2020). https://doi.org/10.1007/s10694-020-00989-9.

[27] N. Elhami-Khorasani, E. Castillo, Juan Gustavo Salado Saula, T. Josephs, G. Nurlybekova, Digitized Fuel Load Survey Methodology Using Machine Vision, 2019.

[28] N. Elhami-Khorasani, J.G. Salado Castillo, E. Saula, T. Josephs, G. Nurlybekova, T. Gernay, Application of a Digitized Fuel Load Surveying Methodology to Office Buildings, Fire Technol. (2020). https://doi.org/10.1007/s10694-020-00990-2.

[29] S.E. Magnusson and S. Thelandersson, Temperature-Time Curves of Complete Process of Fire Development. Theoretical Study of Wood Fuel Fires in Enclosed Spaces, Civ. Eng. Build. Constr. Ser. No. 65. Acta Polyt (1970).

[30] J.A. Rockett, Fire Induced Gas Flow in an Enclosure, Combust. Sci. Technol. 12 (1976) 165–175.

[31] P.H. Thomas, A.J.M. Heselden, Fully Developed Fires in Single Compartments, Fire Res. Note No. 923, Fire Res. Station. Borehamwood, UK. (1962).

[32] T.Z. Harmathy, Design of buildings for fire safety — Part I, Fire Technol. 12 (1976) 95–108. https://doi.org/10.1007/BF02629478.

[33] T.Z. Harmathy, A new look at compartment fires, part I, Fire Technol. 8 (1972) 196–217. https://doi.org/10.1007/BF02590544.

[34] T.Z. Harmathy, Design of buildings for life safety — Part II, Fire Technol. 12 (1976) 219–236. https://doi.org/10.1007/BF02624797.

[35] J.L. Torero, A.H. Majdalani, A.E. Cecilia, A. Cowlard, Revisiting the compartment fire, Fire Saf. Sci. 11 (2014) 28–45. https://doi.org/10.3801/IAFSS.FSS.11-28.

[36] B.J. McCaffrey, J.G. Quintiere, M.F. Harkleroad, Estimating room temperatures and the likelihood of flashover using fire test data correlations, Fire Technol. 17 (1981) 98–119. https://doi.org/10.1007/BF02479583.

[37] K.L. Foote, P.J. Pagni, N.J. Alvares, Tempera- ture Correlations for Forced-Ventilated Compartment Fires, in: Proc. First Int. Symp. Int. Assoc. Fire Saf. Sci., Hemisphere Publishing, Newport, Australia, 1986: pp. 139–148.

[38] C. Beyler, Analysis of Compartment Fires with Forced Ventilation, in: Fire Saf. Sci. Proc. Third Int. Symp. Elsevier Sci., New York, 1991: pp. 291–300.

[39] M. Peatross, C. Beyler, Thermal Environment Prediction In Steel-bounded Preflashover Compartment Fires, Fire Saf. Sci. 4 (1994) 205–216. https://doi.org/10.3801/iafss.fss.4-205.

[40] V. Babrauskas, A closed-form approximation for post-flashover compartment fire temperatures, Fire Saf. J. 4 (1981) 63–73. https://doi.org/10.1016/0379-7112(81)90005-9.

[41] M. Law, Structural Engineering, 1 (1983) 25.

[42] V. Babrauskas, C0MPF2 -A Program for Calculating Post-Flashover Fire Temperatures, 1979.

[43] A. Jowsey, J. Torero, B. Lane, Heat Transfer to the Structure during the Fire, in: Dalmarnock Fire Tests Exp. Model., School of Engineering and Electronics, University of Edinburgh, 2007.

[44] K. Kawagoe, T. Sekine, Estimation of Fire Temperature-Time Curve in Rooms, Tokyo, 1963.

[45] K. Odeen, Experimental and Theoretical Study of processes of Fire Development in Building :

Report 23, 1968.

[46] W. Sjolin, Fires in Residential Spaces Ignited by Heat Radiation from Nuclear Weapons, 1969.

[47] C. Ahlquist, S. Thelandersson, Description and Evaluation of Full-Scale Fire Tests Made by National Swedish Institute fof Material Testing, Lund Insitute of Technology, 1968.

[48] L. Fox, Numerical Solution of Ordinary and Partial Differential Equations, 1963.

[49] O. Pettersson, S.E. Magnusson, J. Thor, Fire Engineering Design of Steel Structures. Bulletin 52, 1976.

[50] J. Gales, B. Chorlton, C. Jeanneret, The Historical Narrative of the Standard Temperature–Time Heating Curve for Structures, Fire Technol. (2020). https://doi.org/10.1007/s10694-020-01040-7.

[51] K. Hertz, Assessment of performance-based requirements for structural design, Fire Saf. Sci. (2005) 315–325. https://doi.org/10.3801/IAFSS.FSS.8-315.

[52] J.M. Franssen, Improvement of the Parametric Fire of Eurocode 1 based on Experimental Test Results, in: Fire Saf. Sci. – Proc. Sixth Int. Symp., France, n.d.: pp. 927–938.

[53] Y. Hasemi, Y. Yokobayashi, T. Wakamatsu, A. V. Ptchelintsev, Modelling of heating mechanism and thermal response of structural components exposed to localised fires.Thirteenth Meeting of the UJNR Planel on Fire Research and Safety, 1996.

[54] A. Pchelintsev, Y. Hasemi, T. Wakamatsu, Y. Yokobayashi, Experimental And Numerical Study On The Behaviour Of A Steel Beam Under Ceiling Exposed To A Localized Fire, in: Fire Saf. Sci. – Proc. Fifth Int. Symp. Melbourne, 3-7 March, 1997: p. Fire Safety Science 5: 1153-1164. https://doi.org/10.3801/IAFSS.FSS.5-1153.

[55] D. Kamikawa, Y. Hasemi, K. Yamada, Nakamura, Mechanical response of a steel column exposed to a localized fire., in: Proc. Fourth Int. Work. Stuctures Fire, Aveiro, Port., 2006: p. pp 225–234.

[56] T. Wakamatsu, Y. Hasemi, Heating Mechanism of Building Components Exposed to a Localized Fire -FDM Thermal Analysis of a Steel Beam under Ceiling-, Int. Assoc. Fire Saf. Sci. (1997) 335–346.

[57] J.-M.M. Franssen, L.-G. Cajot, J.-B. Schleich, Natural Fires in Large Compartments, 1998.

[58] X. Dai, L. Jiang, J. Maclean, S. Welch, A. Usmani, A conceptual framework for a design travelling fire for large compartments with fire resistant islands, in: Proc. 14th Int. Interflam Conf., 2016: pp. 1039–1059.

[59] X. Dai, Y. Jiang, L. Jiang, S. Welch, A.S. Usmani, Implementation of fire models in OpenSees, Proc. 1st Eur. Conf. OpenSees. (2017) 47–50.

[60] J.G. Quintiere, Fundamental of Fire Phenomena, John Wiley, New York, 2006. https://doi.org/10.1002/0470091150.

[61] A.S. Usmani, Y.C. Chung, J.L. Torero, HOW DID THE WTC TOWERS COLLAPSE: A NEW THEORY, Fire Saf. J. 38 (2003) 501–533. https://doi.org/https://doi.org/10.1016/S0379-7112(03)00069-9.

[62] NIST, NIST NCSTAR 1: Final Report on the Collaps of the World Trade Centre Towers, 2005.

[63] R. Friedman, An international survey of computer models for fire and smoke, J. Fire Prot. Eng. 4 (1992) 81–92.

[64] S.M. Olenick, D.J. Carpenter, An updated International survey of computer models for fire and smoke, J. Fire Prot. Eng. 13 (2003) 87–110. https://doi.org/10.1177/104239103033367.

[65] H.E. Mitler, J.A. Rockett, User's Guide to FIRST, A Comprehensive Single-Room Fire Model, CIB W14/88/22, Gaithersburg, MD, n.d.

[66] J.F. Cadorin, J.M. Franssen, A tool to design steel elements submitted to compartment fires - OZone V2. Part 1: Pre- and post-flashover compartment fire model, Fire Saf. J. 38 (2003) 395–427. https://doi.org/10.1016/S0379-7112(03)00014-6.

[67] G.P. Forney, Computing Radiative Heat Transfer Occuring in a Zone Fire Model, Fire Sci. Technol. 14 (1994) 31–47.

[68] J. Stern-Gottfried, G. Rein, Travelling fires for structural design-Part II: Design methodology, Fire Saf. J. 54 (2012) 96–112.

[69] G. Rein, J.L. Torero, W. Jahn, J. Stern-Gottfried, N.L. Ryder, S. Desanghere, M. Lázaro, F. Mowrer, A. Coles, D. Joyeux, D. Alvear, J.A. Capote, A. Jowsey, C. Abecassis-Empis, P. Reszka, Round-robin study of a priori modelling predictions of the Dalmarnock Fire Test One, Fire Saf. J. 44 (2009) 590–602. https://doi.org/10.1016/j.firesaf.2008.12.008.

[70] British Steel plc,The Behavior of Multi-Story Steel Framed Buildings in Fire, 1999.

[71] A.M. Jonsdottir, G. Rein, Out of range, Fire Risk Manag. (2009) 14–17. https://doi.org/10.5749/minnesota/9780816676262.003.0005.

[72] B.R. Kirby, D.E. Wainman, L.N. Tomlinson, T.R. Kay, B.N. Peacock, Natural Fires in Large Scale Compartments, Int. J. Eng. Performance-Based Fire Codes. 1 (1999) 43–58.

[73] British Steel, The behavior of multi storey steel framed buildings in fire'. A European Joint Research Program, 1999.

[74] X. Dai, S. Welch, A. Usmani, A critical review of "travelling fire" scenarios for performance-based structural engineering, Fire Saf. J. 91 (2017) 568–578. https://doi.org/10.1016/j.firesaf.2017.04.001.

[75] C. Clifton, Fire Models for Large Firecells, Auckland, New Zealand, 1996.

[76] P.J. Moss, G.C. Clifton, Modelling of the cardington LBTF steel frame building fire tests, Fire Mater. 28 (2004) 177–198.

[77] A.H. Majdalani, J.E. Cadena, A. Cowlard, F. Munoz, J.L. Torero, Experimental characterisation of two fully-developed enclosure fire regimes, Fire Saf. J. 79 (2015) 10–19. https://doi.org/10.1016/j.firesaf.2015.11.001.

[78] G. Rein, X. Zhang, P. Williams, B. Hume, A. Heise, A. Jowsey, B. Lane, J.. Torero, Multi-storey fire analysis for high-rise buildings, in: Proc. 11th Int. Interflam Conf., London, UK, 2007: pp. 605–616.

[79] R.L. Alpert, Calculation of Response Time of Ceiling-mounted Fire Detectors, Fire Technol. 8 (1972) 182–195.

[80] X. Dai, S. Welch, O. Vassart, K. Cábová, L. Jiang, J. Maclean, G.C. Clifton, A. Usmani, An extended travelling fire method framework for performance-based structural design, Fire Mater. 44 (2020) 437–457. https://doi.org/10.1002/fam.2810.

[81] J. Franssen, A. Gamba, M. Charlier, Toward a standardized uniformly distributed cellulosic fire load., in: IFireSS 2019—3rd Int. Fire Saf. Symp. Ottawa, Ontario, Canada., 2019: pp. 1–8.

[82] A.S. Usmani, Y.C. Chung, J.L. Torero, How did the WTC towers collapse: a new theory, Fire Saf. J. 38 (2003) 501–533. https://doi.org/10.1016/s0379-7112(03)00069-9.

[83] J. Torero, J.G. Quintiere, T. Steinhaus, Fire Safety in High-rise Buildings: Lessons Learned from the WTC, Jahresfachtagung der Vereingung zur Forderrung des Deutschen Brandschutzez e., V Dresden Ger. (2002) 1–23.

[84] L. Lim, A.H. Buchanan, P.J. Moss, Restraint of fire-exposed concrete floor systems, Fire Mater. 28 (2004) 95–125. https://doi.org/10.1002/fam.854.

[85] J. Franssen, G. Thomas, SAFIR, (n.d.). https://www.uee.uliege.be/cms/c_2383458/en/safir.

[86] J.Y.R. Liew, K.Y. Ma, Advanced analysis of 3D steel framework exposed to compartment fire, Fire Mater. 28 (2004) 253–267. https://doi.org/10.1002/fam.850.

[87] J.M. Franssen, SAFIR: A thermal/structural program for modeling structures under fire, Eng. J. 42 (2005) 143–150.

[88] L. Jiang, P. Kamath, X. Dai, H. Jiayu, S. Chen, A. Usmani, An integrated tool for performance based engineering of structures in fire, in: Int. J. Numer. Methods Eng. Conf. Performance-Based Life-Cycle Struct. Eng., 2015: pp. 944–952. https://doi.org/10.14264/uql.2016.516.

[89] University of California, OpenSees, (n.d.). http://opensees.berkeley.edu/.

[90] K. Prasad, H.R. Baum, Coupled fire dynamics and thermal response of complex building structures, Proc. Combust. Inst. 30 (2005) 2255–2262. https://doi.org/10.1016/j.proci.2004.08.118.

[91] K. Prasad, B. Howard, Fire Structure Interface and Thermal Response of World Trade Center Towers, 2005.

[92] T.L. Bergman, A.S. Lavine, Fundamentals of Heat and Mass Transfer, John Wiley & Sons, 2017.

[93] A. Jowsey, FIRE IMPOSED HEAT FLUXES FOR STRUCTURAL ANALYSIS, The University of Edinburgh, 2006.

[94] D. Drysdale, An Introduction to Fire Dynamics, John Wiley & Sons, 2011.

[95] U. Wickström, D. Duthinh, K. McGrattan, Adiabatic surface temperature for calculating heat transfer to fire exposed structures, Proc. 11th Int. Interflam Conf. 2 (2007) 943–953.

[96] J. Alos-Moya, I. Paya-Zaforteza, M.E.M. Garlock, E. Loma-Ossorio, D. Schiffner, A. Hospitaler, Analysis of a bridge failure due to fire using computational fluid dynamics and finite element models, Eng. Struct. 68 (2014) 96–110. https://doi.org/10.1016/j.engstruct.2014.02.022.

[97] C. Zhang, A. Usmani, Heat transfer principles in thermal calculation of structures in fire, Fire Saf. J. 78 (2015) 85–95. https://doi.org/10.1016/j.firesaf.2015.08.006.

[98] J.C.G. Silva, A. Landesmann, F.L.B. Ribeiro, Interface model to fire-thermomechanical performance-based analysis of structures under fire conditions, in: Fire Evacuation Model. Tech. Conf. 2014, 2014.

[99] J.L. Torero, Assessing the performance of concrete structures in fires., Concrete. 40 (n.d.) 44–49.

[100] M. Malendowski, Analytical Solution for Adiabatic Surface Temperature (AST), Fire Technol. 53 (2017) 413–420. https://doi.org/10.1007/s10694-016-0585-3.

[101] K. McGrattan, S. Hostikka, R. Mcdermott, J. Floyd, M. Vanella, Fire Dynamics Simulator User's Guide, (2019).

[102] J. Sandström, Thermal Boundary Conditions Based on Field Modelling of Fires, 2013.

[103] G.-Q. Li, C. Zhang, INTEGRATED FIRE-STRUCTURE SIMULATION OF A LOCALZIED FIRE TEST ON A CEILING STEEL BEAM, Adv. Steel Constr. 13 (2017) 132–143. https://doi.org/10.18057/IJASC.2017.13.2.3.

[104] H. Hofmeyer, J. Feenstra, R.A.P. Van Herpen, M. Mahendran, Automated two-way CFD fire - FE thermo-mechanical coupling for global modelling of building structures, NAFEMS World Congr. a World Eng. Simul. (2017).

[105] J. Alos-Moya, I. Paya-Zaforteza, M.E.M. Garlock, E. Loma-Ossorio, D. Schiffner, A. Hospitaler, Analysis of a bridge failure due to fire using computational fluid dynamics and finite element models, Eng. Struct. 68 (2014) 96–110. https://doi.org/10.1016/j.engstruct.2014.02.022.

[106] A. Hamins, K. Mcgrattan, K. Prasad, A. Maranghides, T. Mcallister, Experiments And Modeling Of Unprotected Structural Steel Elements Exposed To A Fire, Fire Saf. Sci. 8 (2008) 189–200. https://doi.org/10.3801/iafss.fss.8-189.

[107] D. Pantousa, E. Mistakidis, Interface modelling between CFD and FEM analysis: The dual-layer post-processing model, Eng. Comput. (Swansea, Wales). 34 (2017) 1166–1190. https://doi.org/10.1108/EC-06-2015-0146.

[108] D. Banerjee, W. Hess, T. Olano, J. Terrill, J. Gross, Visualization of structural behavior under fire, U.S. Dep. Commer. (2009) 1–28. http://math.nist.gov/mcsd/savg/papers/VisualizationFire-2009.pdf.

[109] F. Pesavento, M. Pachera, B.A. Schrefler, D. Gawin, A. Witek, Coupled numerical simulation of fire in tunnel, AIP Conf. Proc. 1922 (2018). https://doi.org/10.1063/1.5019085.

[110] J.C.G. Silva, A. Landesmann, F.L.B. Ribeiro, Fire-thermomechanical interface model for performance-based analysis of structures exposed to fire, Fire Saf. J. 83 (2016) 66–78. https://doi.org/10.1016/j.firesaf.2016.04.007.

[111] C. Zhang, J.G. Silva, C. Weinschenk, D. Kamikawa, Y. Hasemi, Simulation Methodology for Coupled Fire-Structure Analysis: Modeling Localized Fire Tests on a Steel Column, Fire Technol. 52 (2016) 239–262. https://doi.org/10.1007/s10694-015-0495-9.

[112] M. Malendowski, A. Glema, Development and Implementation of Coupling Method for CFD-FEM Analyses of Steel Structures in Natural Fire, in: 11th Int. Conf. Mod. Build. Mater. Struct. Tech. MBMST, 2016: pp. 692–700. https://doi.org/10.1016/j.proeng.2017.02.082.

[113] S. Welch, S. Miles, S. Kumar, T. Lemaire, A. Chan, FIRESTRUC - Integrating advanced three-dimensional modelling methodologies for predicting thermo-mechanical behaviour of steel and composite structures subjected to natural fires, Fire Saf. Sci. (2008) 1315–1326. https://doi.org/10.3801/IAFSS.FSS.9-1315.

[114] D. Duthinh, K. McGrattan, A. Khaskia, Recent advances in fire-structure analysis, Fire Saf. J. 43 (2008) 161–167. https://doi.org/10.1016/j.firesaf.2007.06.006.

[115] H.R. Baum, Simulating fire effects on complex building structures, Fire Saf. Sci. 38 (2010) 3–18. https://doi.org/10.3801/IAFSS.FSS.8-3.

[116] N. Tondini, O. Vassart, J. Franssen, Development of an Interface Between Cfd and Fe Software, 7th Int. Conf. Struct. Fire. (2012) 459–468.

[117] N. Tondini, A. Morbioli, O. Vassart, S. Lechêne, J.M. Franssen, An integrated modelling strategy between a CFD and an FE software: Methodology and application to compartment fres, J. Struct. Fire Eng. (2016). https://doi.org/10.1108/JSFE-09-2016-015.

[118] N. Tondini, A. Morbioli, O. Vassart, S. Lechêne, J.-M. Franssen, An integrated modelling strategy between a CFD and an FE software, J. Struct. Fire Eng. 7 (2017) 217–233. https://doi.org/10.1108/jsfe-09-2016-015.

[119] F. Pesavento, M. Pachera, B.A. Schrefler, D. Gawin, A. Witek, Coupled numerical simulation of fire in tunnel, AIP Conf. Proc. 1922 (2018). https://doi.org/10.1063/1.5019085.

[120] F. Pesavento, B.A. Schrefler, D. Gawin, J. Principe, Fully coupled numerical simulation of fire in tunnels: From fire scenario to structural response, MATEC Web Conf. 6 (2013) 5005. https://doi.org/10.1051/matecconf/20130605005.

[121] J.C.G. Silva, A. Landesmann, F.L.B. Ribeiro, Fire-thermomechanical interface model for performance-based analysis of structures exposed to fire, Fire Saf. J. 83 (2016) 66–78. https://doi.org/10.1016/j.firesaf.2016.04.007.

[122] M. Michałand, A. Glema, Development and Implementation of Coupling Method for CFD-FEM Analyses of Steel Structures in Natural Fire, in: Procedia Eng., 2017. https://doi.org/10.1016/j.proeng.2017.02.082.

[123] L. Pyl, L. Schueremans, W. Dierckx, I. Georgieva, Fire safety analysis of a 3D frame structure based on a full-scale fire test, Thin-Walled Struct. 61 (2012) 204–212. https://doi.org/10.1016/j.tws.2012.03.023.

[124] J.L. Torero, A. Law, C. Maluk, Defining the thermal boundary condition for protective structures in fire, Eng. Struct. 149 (2017) 104–112. https://doi.org/10.1016/j.engstruct.2016.11.015.

[125] OpenFIRE, OpenSEES for Fire, http://openseesforfire.github.io/openfire.html, (n.d.). http://openseesforfire.github.io/openfire.html.

[126] B. Merci, T. Beji, Fluid mechanics aspects of fire and smoke dynamics in enclosures, 2016. https://doi.org/10.1201/b21320.

[127] L.S. da Silva, A. Santiago, F. Lopes, Design of composite joints for improved fire robustness (Compfire)', Publications Office of the European Union, 2014.

[128] J.P. Hidalgo, A. Cowlard, C. Abecassis-Empis, C. Maluk, A.H. Majdalani, S. Kahrmann, R. Hilditch, M. Krajcovic, J.L. Torero, An experimental study of full-scale open floor plan enclosure fires, Fire Saf. J. 89 (2017) 22–40. https://doi.org/10.1016/j.firesaf.2017.02.002.

[129] J. Degler, A. Eliasson, J. Anderson, D. Lange, D. Rush, A-priori modelling of the Tisova Fire Test as input to the experimental work, First Int. Conf. Struct. Saf. under Fire Blast. (2015) 429–438.

[130] J.P. Hidalgo, T. Goode, V. Gupta, A. Cowlard, C. Abecassis-Empis, J. Maclean, A.I. Bartlett, C. Maluk, J.M. Montalvá, A.F. Osorio, J.L. Torero, The Malveira fire test: Full-scale demonstration of fire modes in open-plan compartments, Fire Saf. J. 108 (2019) 102827. https://doi.org/10.1016/j.firesaf.2019.102827.

[131] T. Wakamatsu, Y. Hasemi, A. V. Ptchelintsev, Heating mechanism of building components exposed to a localized fire - FEM thermal and structural analysis of a steel beam under ceiling -, Proc. Int. Conf. Offshore Mech. Arct. Eng. - OMAE. 2 (1997) 51–58.

[132] A. Buchanan, The challenges of predicting structural performance in fires, Fire Saf. Sci. (2008) 79–90. https://doi.org/10.3801/IAFSS.FSS.9-79.

[133] R.G.G. Thomas J. Ohlemiller, George W. Mulholland, Skandakumar H. Abeyesekere, James J. Filliben, World Trade Center Disaster Fire Tests of Single Office Workstations, NIST Investig. (2005).

[134] J. Liu, K.W. Chow, Determination of fire load and heat release rate for high-rise residential buildings, Procedia Eng. 84 (2014) 491–497. http://dx.doi.org/10.1016/j.proeng.2014.10.460.

[135] M.T. Ahmadi, A.A. Aghakouchak, R. Mirghaderi, S. Tahouni, S. Garivani, A. Shahmari, S. Epackachi, Collapse of the 16-Story Plasco Building in Tehran due to Fire, Springer US, 2020. https://doi.org/10.1007/s10694-019-00903-y.

[136] J.D. DeHaan, D.J. Icove, Kirk's Fire Investigation, Seventh Ed, 2012.

[137] NFPA 921: Guide for Fire and Explosion Investigations, 2017. National.

[138] V. Babrauskas, Ignition Handbook, Fire Safety Science, 2003.

[139] NIST, NIST NCSTAR 1: Final Report on the Collapse of the World Trade Center Building 7, 2008.

[140] J.L. Torero, Fire-induced structural failure: The World Trade Center, New York, Forensic Eng. 164 (2011) 69–77. https://doi.org/10.1680/feng.2011.164.2.69.

[141] R.M. Foster, T.P.S. Reynolds, M.H. Ramage, What is tall timber? Towards the formal classification of timber as a material of tall building design, WCTE 2018 - World Conf. Timber Eng. (2018).

[142] K. Smith, Fire at Austrian motorcycle museum destroys more than 200 vintage bikes, (2021).

[143] NFPA, NFPA 13: Standard for the Installation of Sprinkler Systems, 2019 Edition, (2019).

[144] A. Marty, U. S. Experience with Sprinklers, (2017).